

**NATIONAL ADVISORY COMMITTEE  
FOR AERONAUTICS**

---

**REPORT 948**

**AN APPARATUS FOR VARYING EFFECTIVE DIHEDRAL  
IN FLIGHT WITH APPLICATION TO A STUDY OF  
TOLERABLE DIHEDRAL ON A CONVENTIONAL  
FIGHTER AIRPLANE**

By **WILLIAM M. KAUFFMAN, CHARLES J. LIDDELL, Jr.  
ALLAN SMITH, and RUDOLPH D. VAN DYKE, Jr.**



**1949**



# AERONAUTIC SYMBOLS

## 1. FUNDAMENTAL AND DERIVED UNITS

	Symbol	Metric		English	
		Unit	Abbreviation	Unit	Abbreviation
Length	$l$	meter	m	foot (or mile)	ft (or mi)
Time	$t$	second	s	second (or hour)	sec (or hr)
Force	$F$	weight of 1 kilogram	kg	weight of 1 pound	lb
Power	$P$	horsepower (metric)		horsepower	hp
Speed	$V$	kilometers per hour	kph	miles per hour	mph
		meters per second	mps	feet per second	fps

## 2. GENERAL SYMBOLS

<p><math>W</math> Weight = <math>mg</math></p> <p><math>g</math> Standard acceleration of gravity = <math>9.80665 \text{ m/s}^2</math> or <math>32.1740 \text{ ft/sec}^2</math></p> <p><math>m</math> Mass = <math>\frac{W}{g}</math></p> <p><math>I</math> Moment of inertia = <math>mk^2</math>. (Indicate axis of radius of gyration <math>k</math> by proper subscript.)</p> <p><math>\mu</math> Coefficient of viscosity</p>	<p><math>\nu</math> Kinematic viscosity</p> <p><math>\rho</math> Density (mass per unit volume) Standard density of dry air, <math>0.12497 \text{ kg-m}^{-4}\text{-s}^2</math> at <math>15^\circ \text{ C}</math> and <math>760 \text{ mm}</math>; or <math>0.002378 \text{ lb-ft}^{-4} \text{ sec}^2</math> Specific weight of "standard" air, <math>1.2255 \text{ kg/m}^3</math> or <math>0.07651 \text{ lb/cu ft}</math></p>
---	---

## 3. AERODYNAMIC SYMBOLS

<p><math>S</math> Area</p> <p><math>S_w</math> Area of wing</p> <p><math>G</math> Gap</p> <p><math>b</math> Span</p> <p><math>c</math> Chord</p> <p><math>A</math> Aspect ratio, <math>\frac{b^2}{S}</math></p> <p><math>V</math> True air speed</p> <p><math>q</math> Dynamic pressure, <math>\frac{1}{2} \rho V^2</math></p> <p><math>L</math> Lift, absolute coefficient <math>C_L = \frac{L}{qS}</math></p> <p><math>D</math> Drag, absolute coefficient <math>C_D = \frac{D}{qS}</math></p> <p><math>D_0</math> Profile drag, absolute coefficient <math>C_{D_0} = \frac{D_0}{qS}</math></p> <p><math>D_i</math> Induced drag, absolute coefficient <math>C_{D_i} = \frac{D_i}{qS}</math></p> <p><math>D_p</math> Parasite drag, absolute coefficient <math>C_{D_p} = \frac{D_p}{qS}</math></p> <p><math>C</math> Cross-wind force, absolute coefficient <math>C_C = \frac{C}{qS}</math></p>	<p><math>i_w</math> Angle of setting of wings (relative to thrust line)</p> <p><math>i_t</math> Angle of stabilizer setting (relative to thrust line)</p> <p><math>Q</math> Resultant moment</p> <p><math>\Omega</math> Resultant angular velocity</p> <p><math>R</math> Reynolds number, <math>\rho \frac{Vl}{\mu}</math> where <math>l</math> is a linear dimension (e.g., for an airfoil of 1.0 ft chord, 100 mph, standard pressure at <math>15^\circ \text{ C}</math>, the corresponding Reynolds number is 935,400; or for an airfoil of 1.0 m chord, 100 mps, the corresponding Reynolds number is 6,865,000)</p> <p><math>\alpha</math> Angle of attack</p> <p><math>\epsilon</math> Angle of downwash</p> <p><math>\alpha_0</math> Angle of attack, infinite aspect ratio</p> <p><math>\alpha_i</math> Angle of attack, induced</p> <p><math>\alpha_a</math> Angle of attack, absolute (measured from zero-lift position)</p> <p><math>\gamma</math> Flight-path angle</p>
---	---



---

## REPORT 948

---

# AN APPARATUS FOR VARYING EFFECTIVE DIHEDRAL IN FLIGHT WITH APPLICATION TO A STUDY OF TOLERABLE DIHEDRAL ON A COVENTIONAL FIGHTER AIRPLANE

By WILLIAM M. KAUFFMAN, CHARLES J. LIDDELL, Jr.  
ALLAN SMITH, and RUDOLPH D. VAN DYKE, Jr.

Ames Aeronautical Laboratory  
Moffett Field, California

---

# National Advisory Committee for Aeronautics

*Headquarters, 1724 F Street NW., Washington 25, D. C.*

Created by act of Congress approved March 3, 1915, for the supervision and direction of the scientific study of the problems of flight (U. S. Code, title 50, sec. 151). Its membership was increased from 12 to 15 by act approved March 2, 1929, and to 17 by act approved May 25, 1948. The members are appointed by the President, and serve as such without compensation.

JEROME C. HUNSAKER, Sc. D., Massachusetts Institute of Technology, *Chairman*

ALEXANDER WETMORE, Sc. D., Secretary, Smithsonian Institution, *Vice Chairman*

HON. JOHN R. ALISON, Assistant Secretary of Commerce.  
DETLEV W. BRONK, Ph. D., President, Johns Hopkins University.  
KARL T. COMPTON, Ph. D., Chairman, Research and Development Board, Department of Defense.  
EDWARD U. CONDON, Ph. D., Director, National Bureau of Standards.  
JAMES H. DOOLITTLE, Sc. D., Vice President, Shell Union Oil Corp.  
R. M. HAZEN, B. S., Director of Engineering, Allison Division, General Motors Corp.  
WILLIAM LITTLEWOOD, M. E., Vice President, Engineering, American Airlines, Inc.  
THEODORE C. LONNQUEST, Rear Admiral, United States Navy, Deputy and Assistant Chief of the Bureau of Aeronautics.

DONALD L. PUTT, Major General, United States Air Force, Director of Research and Development, Office of the Chief of Staff, Matériel.  
JOHN D. PRICE, Vice Admiral, United States Navy, Vice Chief of Naval Operations.  
ARTHUR E. RAYMOND, Sc. D., Vice President, Engineering, Douglas Aircraft Co., Inc.  
FRANCIS W. REICHELDERFER, Sc. D., Chief, United States Weather Bureau.  
HON. DELOS W. RENTZEL, Administrator of Civil Aeronautics, Department of Commerce.  
HOYT S. VANDENBERG, General, Chief of Staff, United States Air Force.  
THEODORE P. WRIGHT, Sc. D., Vice President for Research, Cornell University.

HUGH L. DRYDEN, Ph. D., *Director*

JOHN F. VICTORY, LL. M., *Executive Secretary*

JOHN W. CROWLEY, JR., B. S., *Associate Director for Research*

E. H. CHAMBERLIN, *Executive Officer*

HENRY J. REID, D. Eng., Director, Langley Aeronautical Laboratory, Langley Field, Va.

SMITH J. DEFRAUICE, B. S., Director, Ames Aeronautical Laboratory, Moffett Field, Calif.

EDWARD R. SHARP, Sc. D., Director, Lewis Flight Propulsion Laboratory, Cleveland Airport, Cleveland, Ohio

## TECHNICAL COMMITTEES

AERODYNAMICS  
POWER PLANTS FOR AIRCRAFT  
AIRCRAFT CONSTRUCTION

OPERATING PROBLEMS  
INDUSTRY CONSULTING

*Coordination of Research Needs of Military and Civil Aviation*

*Preparation of Research Programs*

*Allocation of Problems*

*Prevention of Duplication*

*Consideration of Inventions*

LANGLEY AERONAUTICAL LABORATORY  
Langley Field, Va.

LEWIS FLIGHT PROPULSION LABORATORY  
Cleveland Airport, Cleveland, Ohio

AMES AERONAUTICAL LABORATORY  
Moffett Field, Calif.

*Conduct, under unified control, for all agencies of scientific research on the fundamental problems of flight*

OFFICE OF AERONAUTICAL INTELLIGENCE  
Washington, D. C.

*Collection, classification, compilation, and dissemination of scientific and technical information on aeronautics*



## REPORT 948

### AN APPARATUS FOR VARYING EFFECTIVE DIHEDRAL IN FLIGHT WITH APPLICATION TO A STUDY OF TOLERABLE DIHEDRAL ON A CONVENTIONAL FIGHTER AIRPLANE

By WILLIAM M. KAUFFMAN, CHARLES J. LIDDELL, JR., ALLAN SMITH, and RUDOLPH D. VANDYKE, JR.

#### SUMMARY

*An apparatus for varying effective dihedral in flight by means of servo actuation of the ailerons in response to sideslip angle is described. The results of brief flight tests of the apparatus on a conventional fighter airplane are presented and discussed. The apparatus is shown to have satisfactorily simulated a wide range of effective dihedral under static and dynamic conditions. The effects of a small amount of servo lag are shown to be measurable when the apparatus is simulating small negative values of dihedral. However, these effects were not considered by the pilots to give the airplane an artificial feel.*

*The results of an investigation employing the apparatus to determine the tolerable (safe for normal fighter operation) range of effective dihedral on the test airplane are presented. A survey of pilots' opinions was made to determine which values of effective dihedral were intolerable. It was found that small amounts of negative dihedral (of the order of  $-5^\circ$ ) as well as values of positive dihedral greater than  $20^\circ$  could be tolerated by the pilots. It was found, in fact, that at landing-approach speeds an effective dihedral high enough ( $28.4^\circ$ ) to produce oscillatory instability could be tolerated. The occurrence of rolling-velocity reversals during rudder-fixed aileron rolls with high positive values of effective dihedral did not adversely affect the pilots' opinions of the over-all lateral handling characteristics. The relation between the findings of this investigation and the present Air Force-Navy stability and control specifications is discussed.*

#### INTRODUCTION

For many years the NACA has been carrying on research in the field of flying qualities of piloted airplanes. A set of preliminary flying-qualities requirements was published in reference 1. This work and the work of other organizations have led to the formulation of flying-qualities requirements by the military services (references 2 and 3). However, these specifications have, in general, been based on experience with airplanes of conventional configuration and, hence, with more or less conventional handling characteristics. The use of highly swept-back wings, triangular wings, and wings of low aspect ratio for airplanes to be operated at very high speeds and altitudes has introduced stability and control characteristics which hitherto had not been considered in flying-qualities work. A reexamination of certain aspects of the present flying-qualities requirements has, therefore, been initiated. Particular emphasis is being given to the dynamic lateral and directional motions.

As part of this program, flight tests were planned to determine the effects of changes in effective dihedral on the dynamic-stability characteristics of a conventional fighter airplane. An apparatus for varying the effective dihedral in flight was developed, since this procedure was considered necessary to isolate the effects of stability changes on the airplane behavior from those due to other influences such as air gustiness. This apparatus consists essentially of a servomechanism which deflects the ailerons through a differential linkage in proportion to the movement of a sideslip vane. The ability of the apparatus to simulate satisfactorily changes in dihedral of about  $\pm 9^\circ$  at high speeds without great practical difficulty led to minor modifications in order to extend the range to approximately twice this value. The revised apparatus thus permitted simulation of the large dihedral range characteristic of swept, triangular, and low-aspect-ratio plan forms. In order to determine some of the difficulties likely to be encountered with extreme effective dihedral, the apparatus then was employed in a flight investigation to evaluate, from measurements and pilots' opinions, the tolerable limits of effective dihedral for the test airplane.

The description and flight evaluation of the dihedral-effect control apparatus and flight determination of the tolerable range of effective dihedral of the test airplane have been reported previously in references 4 and 5. This report combines this information into one report and includes some additional information.

#### NOTATION

$\Gamma_e$	effective dihedral, degrees
$V$	true airspeed, feet per second
$V_i$	indicated airspeed, knots
$q$	dynamic pressure, pounds per square foot
$S$	wing area, square feet
$b$	wing span, feet
$\delta_a$	total aileron deflection (sum of left and right aileron deflections, left when left aileron is up), degrees
$(\delta_a)_s$	$\delta_a$ due to servo action, degrees
$\delta_r$	rudder deflection, degrees
$\delta_t$	aileron tab deflection (positive when tab located on left aileron is up), degrees
$\theta$	lateral stick deflection, degrees



$F$	lateral stick force, pounds
$\beta$	sideslip angle, degrees
$\varphi$	bank angle, degrees
$p$	rolling velocity, radians per second
$P$	period of oscillation, seconds
$T_{\frac{1}{2}}$	time for oscillation to damp to half amplitude, seconds
$C_{\frac{1}{2}}$	number of cycles for oscillation to damp to half amplitude
$T_2$	time for oscillation to double amplitude, seconds
$C_l$	rolling-moment coefficient $\left(\frac{\text{rolling moment}}{qSb}\right)$
$C_{l\beta}$	rate of change of rolling-moment coefficient with respect to sideslip angle $\left(\frac{\partial C_l}{\partial \beta}\right)$ , per degree
$C_{l\alpha}$	rate of change of rolling-moment coefficient with wing-tip helix angle $\left[\frac{\partial C_l}{\partial (pb/2V)}\right]$
$C_{l\delta}$	rate of change of rolling-moment coefficient with aileron deflection $\left(\frac{\partial C_l}{\partial \delta_a}\right)$ , per degree
$\left(\frac{\partial \delta_a}{\partial \beta}\right)_s$	aileron servo-gearing ratio
$\left(\frac{d\delta_i}{d\delta_a}\right)_s$	aileron tab servo-gearing ratio
$(\Delta C_{l\beta})_s$	change in $C_{l\beta}$ due to servo action, per degree
$\frac{ p }{ \beta }$	ratio of amplitude of rolling velocity to amplitude of sideslip angle of the oscillatory mode, per second
$\frac{ \varphi }{ \beta }$	ratio of amplitude of angle of bank to amplitude of sideslip angle of the oscillatory mode

### DESCRIPTION OF APPARATUS

#### TEST AIRPLANE

The airplane used in the investigation was a conventional propeller-driven, low-midwing, single-place fighter airplane. A three-view drawing of the airplane as instrumented for flight tests is given in figure 1.

#### EFFECTIVE-DIHEDRAL CONTROL APPARATUS

**Theory and design conditions.**—Dihedral effect can be expressed quantitatively by the stability coefficient  $C_{l\beta}$ , the rate of change of rolling-moment coefficient with angle of sideslip. The design of the present apparatus is based on the fact that a change in apparent  $C_{l\beta}$  can be obtained from actuation, by a servomechanism with an output motion  $\delta$  proportional to sideslip angle  $\beta$ , of a control surface which produces rolling moment. Then

$$(\Delta C_{l\beta})_s = C_{l\delta} \left(\frac{\partial \delta}{\partial \beta}\right)_s \quad (1)$$

Preliminary investigation showed that the most practicable method of obtaining large servo-actuated rolling-moment coefficients proportional to sideslip angle on the test airplane was by use of the normal ailerons. In order to simulate changes in  $C_{l\beta}$ , the servo motion of the ailerons should not be accompanied by any resultant movement of the stick or increment in lateral stick force. This condition arises from

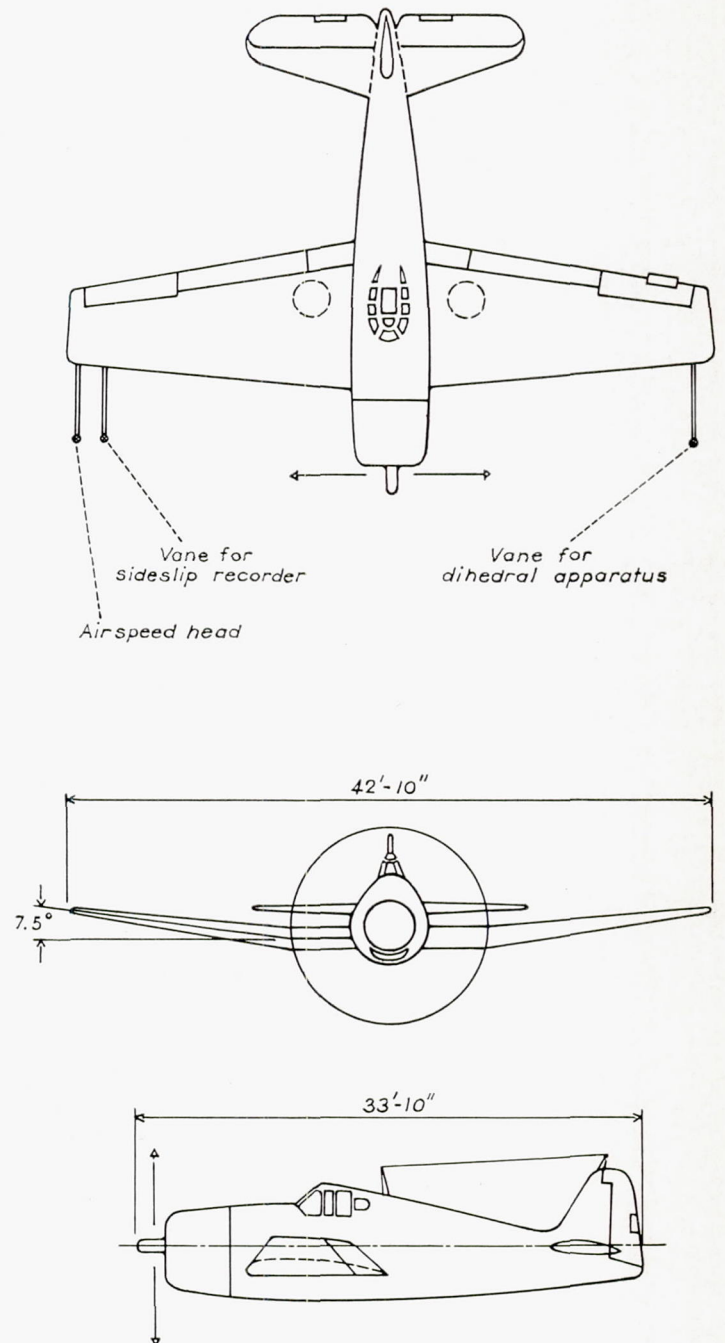


FIGURE 1.—Three-view drawing of the test airplane. Wing area, 334 sq ft; aspect ratio, 5.5; taper ratio, 0.5.

the fact that the aileron stick-deflection and stick-force gradients  $d\theta/d\beta$  and  $dF/d\beta$  required for balance in steady straight sideslips are, to a pilot, measures of the stick-fixed and stick-free dihedral effect. In order to obtain changes in  $d\theta/d\beta$  and apparent stick-fixed  $C_{l\beta}$ , a differential linkage is required in the control system, with aileron deflection as the output and pilot-applied stick motion and an independent servo motion as inputs. The maximum value of servo-gear ratio  $(\partial \delta_a / \partial \beta)_s$  which then can be utilized is restricted in two ways: First, the maximum servo-actuated aileron deflection must be limited to allow the pilot sufficient aileron deflection for normal maneuvering and emergency control; and, second, the sideslip-angle range over which the apparatus is operative for any servo-gear ratio must be greater than that encountered during the desired maneuvers. These restrictions



become more severe as airspeed is decreased, since both the pilot-required aileron control and the sideslip-angle range then generally increase.

In order to obtain changes in  $dF/d\beta$  and apparent stick-free  $C_{l\beta}$ , a means of canceling the hinge moment due to servo-actuated deflection of the ailerons is required, since with common differential linkages the entire hinge moment is transmitted back to the stick. It was desired for the first tests that the ratio of the stick-free value of  $C_{l\beta}$  to the stick-fixed value remain constant as the stick-fixed value was changed. This leads to the requirement that the stick-free value be zero when the stick-fixed value is zero, which is equivalent to assuming that the change in aileron hinge moment with sideslip is zero. The desired effect is approximated on the present installation by servo actuation of the aileron trim tab to furnish an aileron hinge moment equal and opposite to that arising from the servo-actuated aileron motion. As was the case for the aileron system, a differential gearing with tab angle as the output motion and the tab servo and pilot-actuated trim-tab motions as inputs is required.

Although the discussion thus far has been confined to the static flight condition of steady straight sideslips, a similar explanation which yields similar requirements can be developed for maneuvers in which sideslip angle varies rapidly. The ideal servomechanism for producing a change in  $C_{l\beta}$  which is constant under any dynamic condition would be one with an output motion always in phase with, and a constant proportion of, the input quantity. Deviations of actual servomechanisms from this ideal cause undesired variations in  $C_{l\beta}$ .

**Aileron drive system.**—There are a number of mechanisms which will give the desired differential aileron motion, and the choice between them depends on the particular control system under consideration. The linkage which was used for the test airplane is illustrated schematically in figure 2. In the original aileron circuit, lateral stick motion imparted a corresponding angular motion to a control horn attached to the forward end of a torque tube which was supported by two fixed bearings. This rotation was transmitted as a linear motion by push rods attached by self-aligning bearings to the horn. In the modified installation an additional torque-tube bearing was attached to the fuselage structure just forward of the stick. The torque tube was cut immediately forward of this bearing and a universal joint installed. The original forward fixed bearing was replaced by two bearings. The one nearest the torque-tube horn restrains the tube vertically by means of roller guides but permits the tube to rotate in a horizontal plane about the vertical axis of the universal joint. The second bearing is bolted to a plate which is also free to rotate in a horizontal plane about the vertical axis of the universal joint. This plate is attached by cables to a drum on the servo motor and rotates in a horizontal plane when the drum rotates. Thus, the forward portion of the torque tube swings about the universal joint when the servo responds to a sideslip signal. The torque-tube horn and the aileron push rods then move laterally if the stick is held fixed, and this motion results in an aileron deflection proportional to drum rotation. The

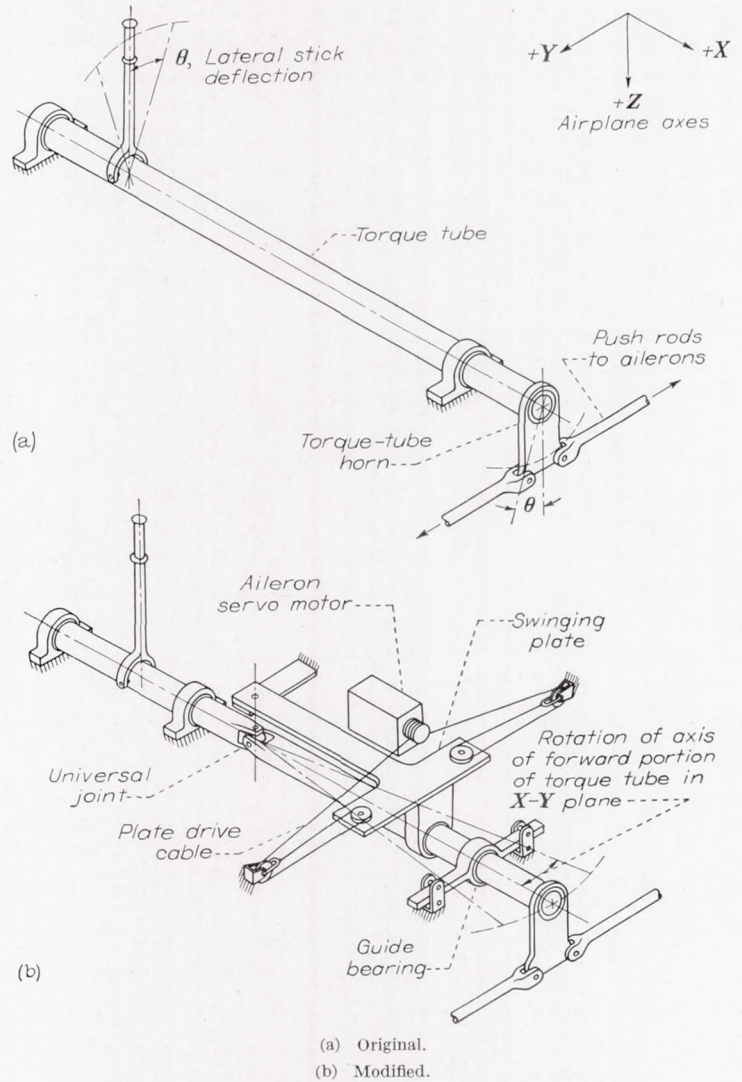


FIGURE 2.—Sketch of original and modified aileron-control system.

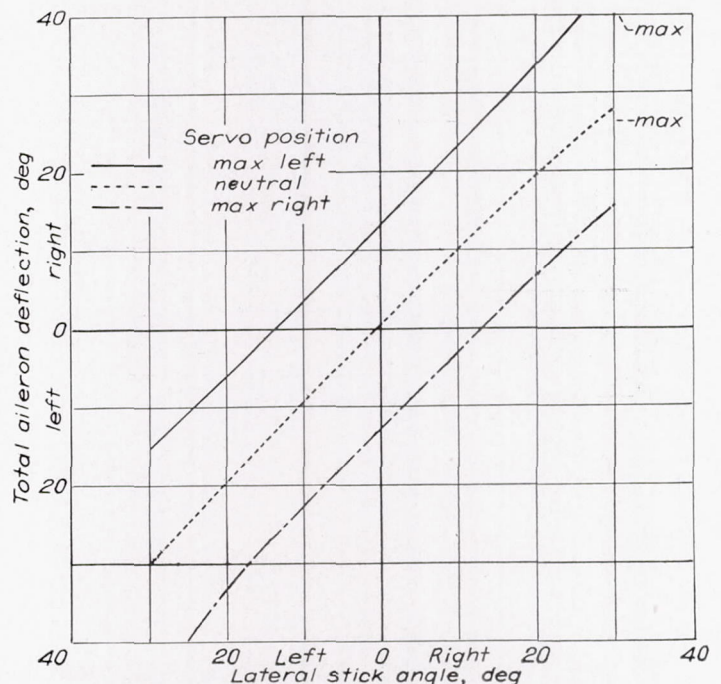


FIGURE 3.—Kinematics of aileron-control system for various servo positions.



pilot still can apply in the normal manner any additional desired aileron deflection up to the maximum in either direction. The kinematics of the revised system are shown in figure 3, in which total aileron deflection  $\delta_a$  (the sum of left and right aileron angles) is plotted as a function of lateral stick deflection  $\theta$  for neutral and maximum test servo positions. These curves and additional data obtained at intermediate servo positions showed that, as is desired, the gearings  $\partial\delta_a/\partial\theta$  and  $(\partial\delta_a/\partial\beta)_s$  are nearly constant over the available ranges of  $\delta_a$  and  $\theta$ .

**Aileron servomechanism.**—The aileron and tab servomechanisms were developed from an electric amplidyne system normally used for remote control of aircraft gun turrets. This system was chosen on the basis of signal-system and motor-output requirements, applicability to aircraft, and availability. A simplified electrical circuit diagram of the installation is given in figure 4. The error-measuring portion of the aileron servomechanism is essentially a two-potentiometer bridge circuit with a 30-volt 400-cycle power supply. One potentiometer is geared mechanically to a yaw vane located on a boom extending forward from the left wing tip of the airplane. The second potentiometer is connected to the aileron servo motor. With the yaw vane

and servo motor initially neutral, the bridge circuit is at one balance point. When the vane is deflected through an angle of sideslip  $\beta$ , an error signal is supplied by the bridge to the amplifier. The amplified signal, converted to direct current, is fed to the field of an amplidyne generator, the armature of which is driven continuously at constant speed by the direct-current amplidyne motor. The general output voltage, of a polarity and magnitude determined by the error signal, is applied to the armature of the reversible separately excited direct-current aileron servo motor. The generator output voltage determines the direction and speed of the servo-motor rotation, which moves the torque tube and attached potentiometer in the direction which tends to balance the bridge circuit at a new point corresponding to  $\beta$  and  $(\delta_a)_s$ . The servo gearing  $(\partial\delta_a/\partial\beta)_s$  can be altered through the switch  $S_1$ , which in effect varies the bridge unbalance voltage per degree sideslip. The sign of  $(\partial\delta_a/\partial\beta)_s$ , and thus  $(\Delta C_{l\beta})_s$ , can be reversed by switch  $S_2$ .

**Aileron tab drive and servomechanism.**—The ratio  $(d\delta_t/d\delta_a)_s$  of the tab motion to aileron motion required to balance the hinge moment due to servo-actuated aileron motion was determined from preliminary flight tests. Insufficient total power of the original trim tab necessitated

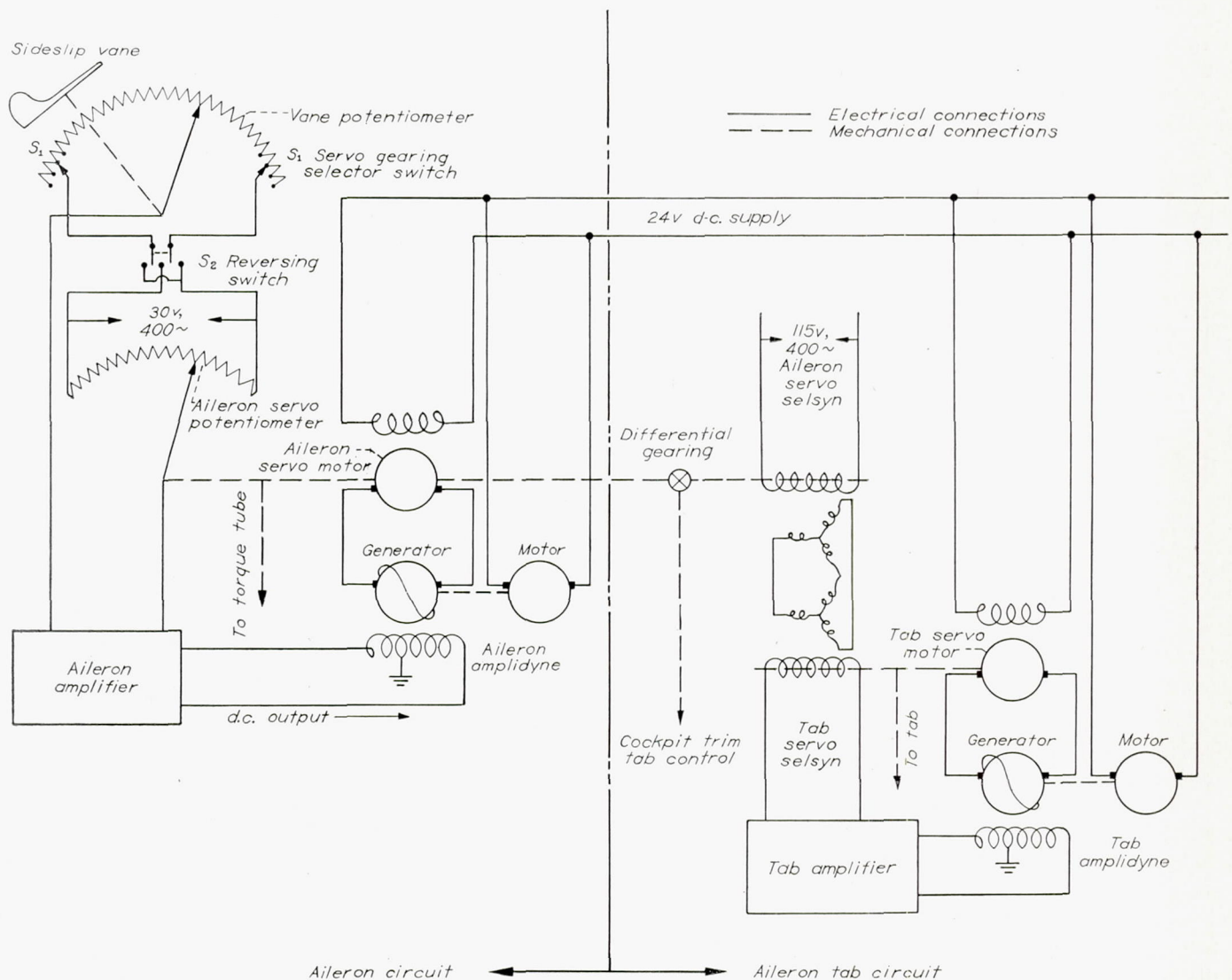


FIGURE 4.—Simplified electrical circuit diagram of the effective-dihedral control apparatus.



an increase of both the area and the control throw of the tab, which was located on the left aileron. Brief flight tests with this revised tab yielded a value of  $(d\delta_t/d\delta_a)_s$  of  $-1.15$ , which was used for the present tests. Although the standard aileron trim-tab drive linkages passed near the aileron servo-motor location in the cockpit, it was not possible to utilize this servo motor in obtaining the desired tab action  $(d\delta_t/d\delta_a)_s$  because of excessive lost motion in the tab linkages between cockpit and tab surface. Therefore, a separate servo motor was installed in the left wing to drive the tab more directly. As indicated by figure 4, the tab servo electrical circuit is similar to the aileron circuit, although selsyns are used in place of potentiometers in the signal network. Error signals arising from rotation of the selsyn attached to the aileron servo result in motions of the tab servo and selsyn which tend to reduce the error to zero. The pilot is furnished with a trim-tab control which, when rotated, acts through differential gearing to rotate the aileron motor selsyn and, hence, the aileron tab.

**Servomechanism controls and operating procedure.**—The location of the aileron drive system and associated cockpit

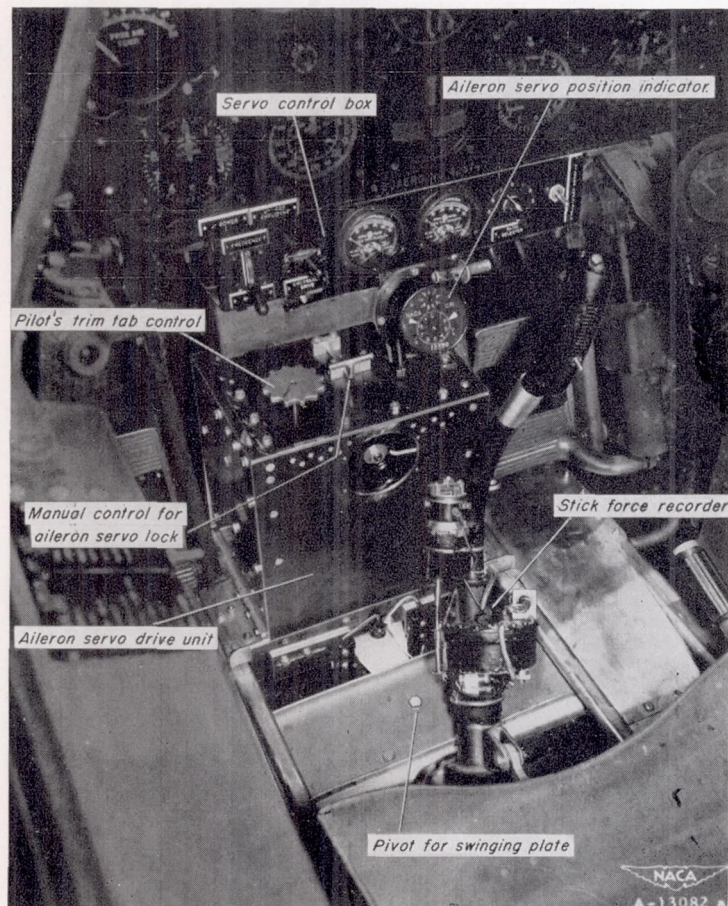


FIGURE 5.—View of cockpit interior showing aileron servo-drive and control components.

controls is shown in figure 5. When the apparatus is operated in flight, the error-signal circuits are energized first. The desired value of  $(\partial\delta_a/\partial\beta)_s$  then is set with the servo-gearing ratio-selector switch, which gives values ranging from maximum positive to maximum negative in six approximately equal increments. The use of ammeters which indicate the aileron servo error signal reduce the possibility

of abrupt motions which might occur if the servomotor were energized with the airplane at a sizable angle of sideslip. The pilot, by use of the rudder, reduces the error signal to zero and then places the entire system in operation by switching on the aileron amplidyne. Changes in  $C_{l\beta}$  then are easily obtainable at any time by reducing the sideslip angle to zero and moving the servo-gearing selector switch. Both the aileron and the tab drives are equipped with limit switches and with locking and emergency drive circuits which permit the pilot to lock or return to neutral the torque tube and tab in the event of malfunctioning.

## INSTRUMENTATION

Standard NACA photographically recording instruments were used to measure as a function of time the following variables: indicated airspeed; pressure altitude, applied aileron control force; angular positions of the aileron surfaces, aileron tab, aileron servo drum, forward portion of the aileron torque tube in the horizontal plane, rudder, and stick; sideslip angle; and airplane rolling and yawing velocities. A free-swivelling pitot-static head mounted on a boom extending forward from the right wing tip was used for airspeed and altitude measurements. The recording sideslip vane was mounted on a boom from the right wing at approximately the same location relative to the wing as the vane on the left wing tip for the dihedral apparatus. (See fig. 1.)

## I. EVALUATION OF THE EFFECTIVE-DIHEDRAL CONTROL APPARATUS

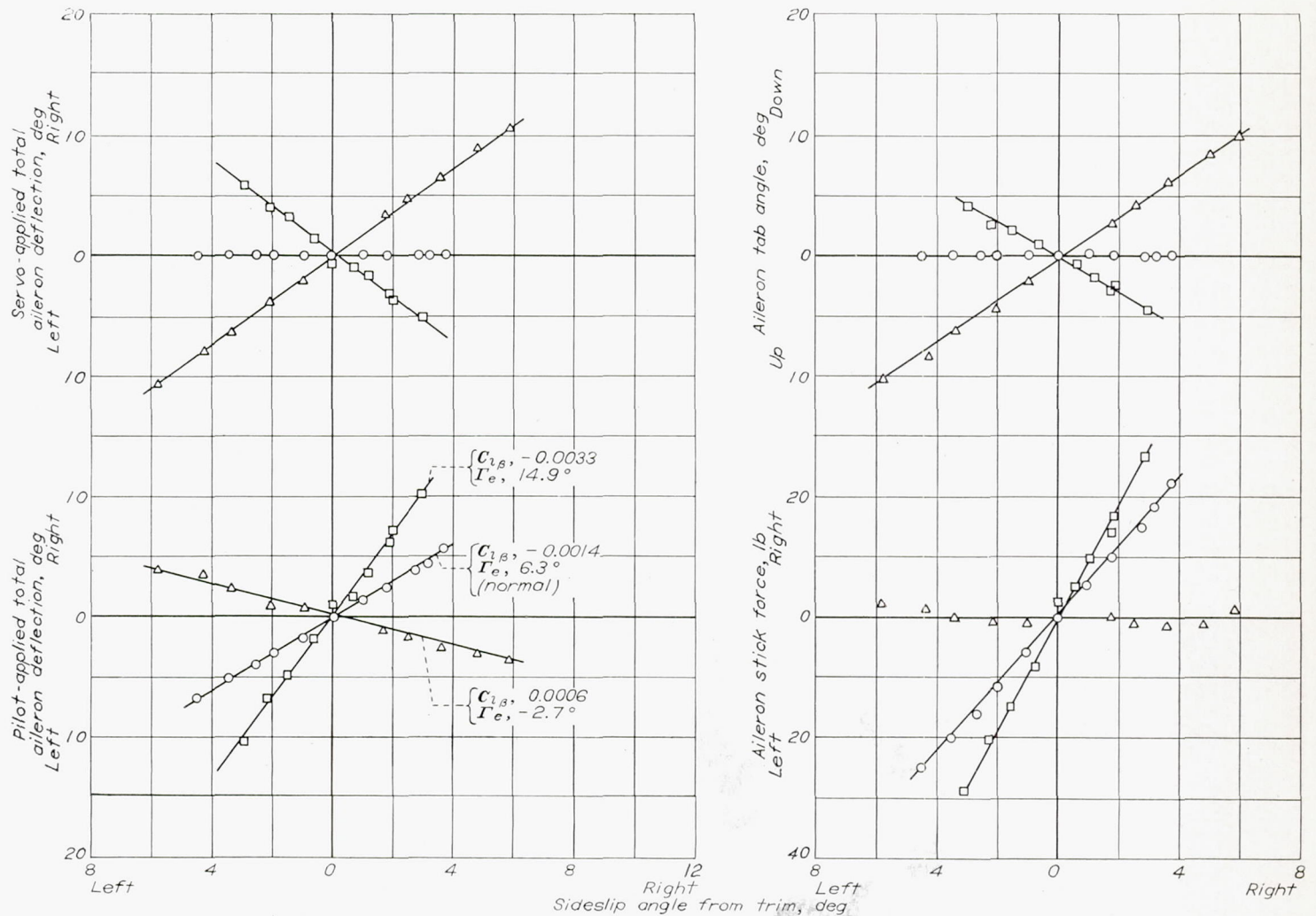
The results presented in this part of the report are based on data obtained during the first flights of the test airplane made with the complete effective-dihedral control apparatus in operation. The primary purpose of these early tests was to determine, from recorded data and pilots' opinions, the ability of the apparatus to simulate changes in stick-fixed and stick-free dihedral effect under static and dynamic flight conditions.

### TESTS AND RESULTS

Although data were obtained at several airspeeds and values of servo gearing  $(\partial\delta_a/\partial\beta)_s$ , results presented herein are confined to the normal airplane (servo inoperative) and to the maximum initial test values of  $(\partial\delta_a/\partial\beta)_s$  or  $(\Delta C_{l\beta})_s$  at a nominal indicated airspeed of 300 knots. The data presented are typical, and these test conditions approximate those originally considered in the design of the apparatus. Operation under static flight conditions was studied in steady straight sideslips and under dynamic conditions in abrupt rudder kicks and cockpit-controls-fixed lateral oscillations.

**Steady straight sideslips.**—The aileron and tab deflections supplied by servo action and the net balancing aileron deflection and stick force supplied by the pilot are plotted in figure 6 as a function of sideslip angle for the three test servo-gearing ratios. All quantities represent changes from the wings-level trim condition. Corrections for distortion in the aileron servo drive system (between the aileron servomotor and the torque tube) have been made.



FIGURE 6.—Lateral control characteristics in steady straight sideslips.  $V_i=300$  knots.

The following formula was used in computing the values of stick-fixed  $C_{l_{\beta}}$  noted in figure 6

$$C_{l_{\beta}} = C_{l_p} \left[ \frac{d(pb/2V)}{d\delta_a} \right] \left( \frac{\partial \delta_a}{\partial \beta} \right) \quad (2)$$

where a value of  $C_{l_p}$  of  $-0.45$  was obtained from reference 6. Abrupt rudder-fixed aileron-roll flight tests gave a value of  $-0.00215$  for  $d(pb/2V)/d\delta_a$  (corrected approximately for effects of sideslip), and  $\partial \delta_a / \partial \beta$  is the pilot-applied curve slope from figure 6. Also shown for comparison are values of the stick-fixed effective dihedral angle  $\Gamma_e$  computed from the equation

$$\Gamma_e = \frac{C_{l_{\beta}}}{C_{l_{\beta}}/\Gamma_e} \quad (3)$$

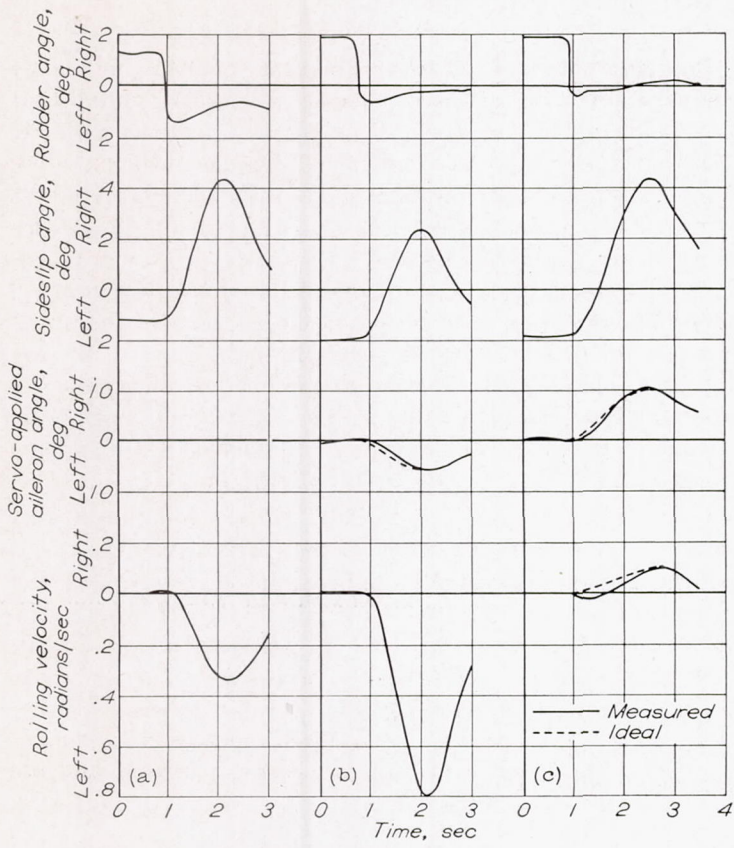
where a value of  $C_{l_{\beta}}/\Gamma_e$  of  $-0.000225$  per degree squared was obtained from reference 6.

**Abrupt rudder kicks.**—The pilot abruptly deflected and held the rudder pedals while the stick was held fixed. Several different rudder deflections, left and right, were employed for each servo-gearing ratio. Typical time histories showing the motions of the control surfaces and airplane are presented in figure 7. The computed aileron deflections due to servo action for an ideal servomechanism (no time lag)

are shown for comparison with the measured values. The variation of the maximum value of the rolling parameter  $pb/2V$  with change in rudder deflection  $\Delta \delta_r$  for these maneuvers is given in figure 8 (a). The ratio of  $pb/2V$  for unit  $\Delta \delta_r$  for each servo-gearing ratio to the value for the normal airplane was computed from the slopes of these curves and is shown in figure 8 (b) as a function of the corresponding static stick-fixed effective dihedral angle. A similar predicted curve computed by the method of reference 7 is shown for comparison.

**Controls-fixed lateral oscillations.**—Lateral oscillations were induced from an initial steady-sideslip attitude by abruptly returning and holding the rudder pedals and control stick in trim position. Typical time histories of the control deflections, including the computed aileron motion supplied by an ideal servomechanism, and resultant airplane motions are given in figure 9. The absolute values of servo-applied aileron deflection shown in figure 9 are probably in error because of initial misalignment at the trim sideslip angle. This factor is not important, however, because only the time variation of this quantity has any significance here. The oscillation period  $P$  and number of cycles to damp to one-half amplitude  $C_{1/2}$  were determined from the time histories of sideslip angle, and are plotted in figure 10 as a function of effective dihedral angle  $\Gamma_e$ . Values





(a)  $\Gamma_e = 6.3^\circ$  (normal, servo inoperative).  
 (b)  $\Gamma_e = 14.9^\circ$ .  
 (c)  $\Gamma_e = -2.7^\circ$ .

FIGURE 7.—Time histories of abrupt, stick-fixed rudder kicks.  $V_i = 300$  knots.

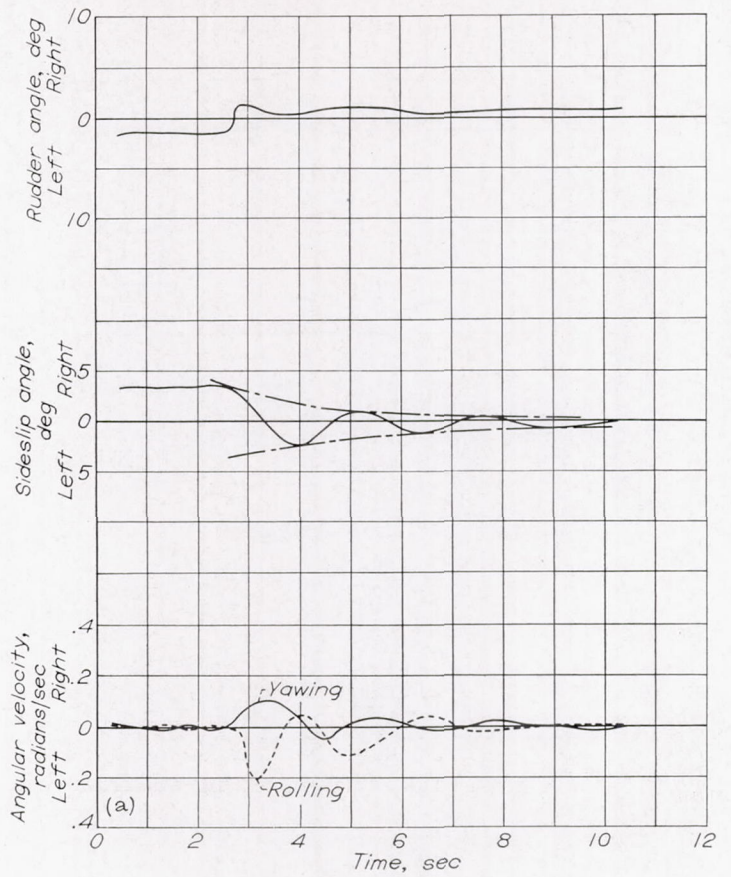
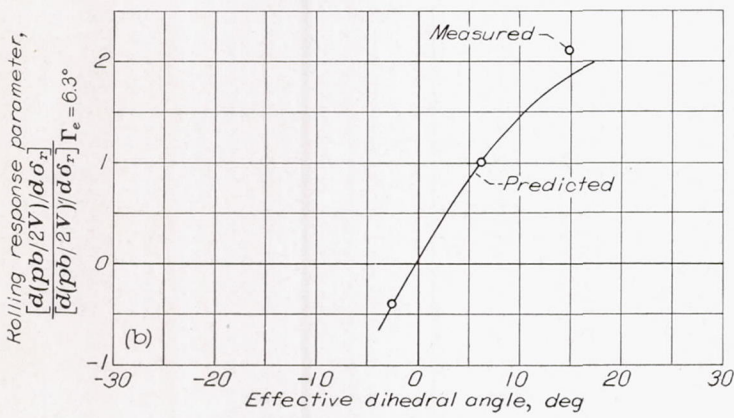
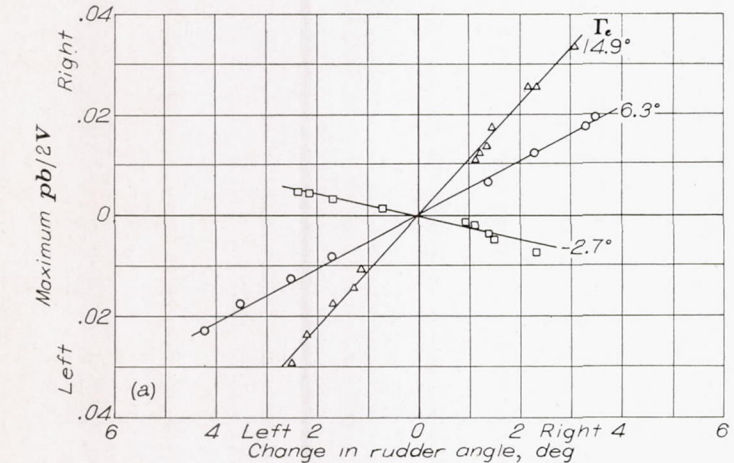
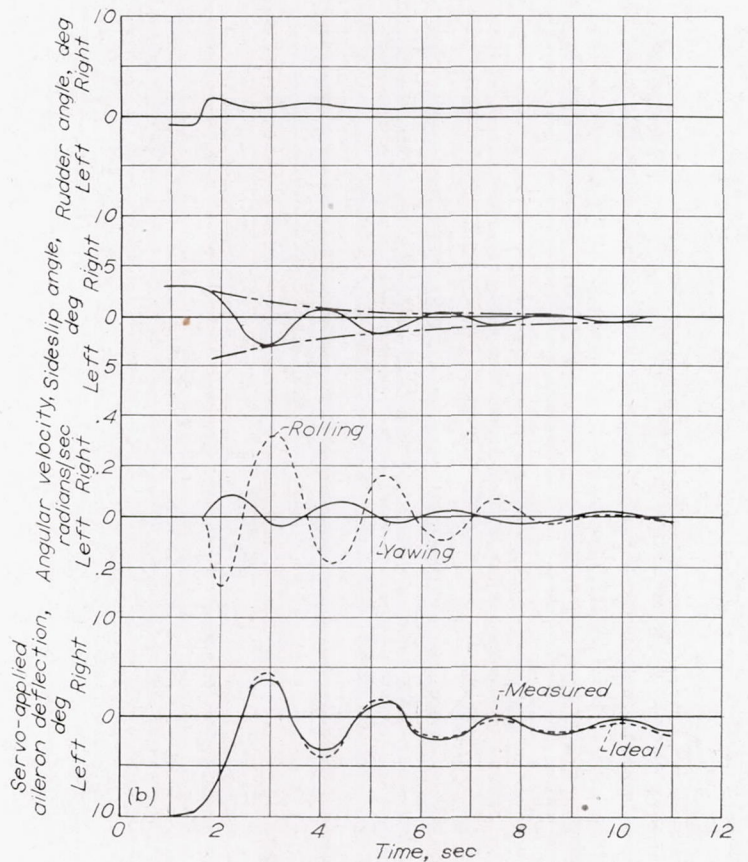


FIGURE 9.—Time histories of lateral oscillations.  $V_i = 300$  knots.



(a) Variation of maximum  $pb/2V$  with  $\Delta \delta_r$ .  
 (b) Variation of rolling response parameter with  $\Gamma_e$ .

FIGURE 8.—Rolling response characteristics in abrupt rudder kicks  $V_i = 300$  knots.



(b)  $\Gamma_e = 14.9^\circ$ .

FIGURE 9.—Continued.



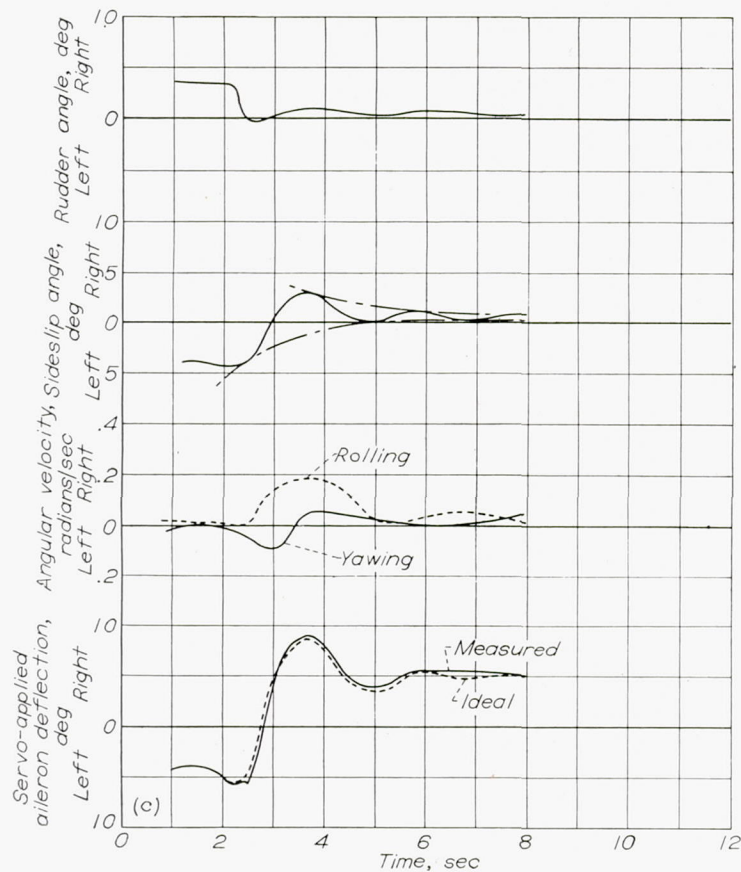
(c)  $\Gamma_e = -2.7^\circ$ .

FIGURE 9.—Concluded.

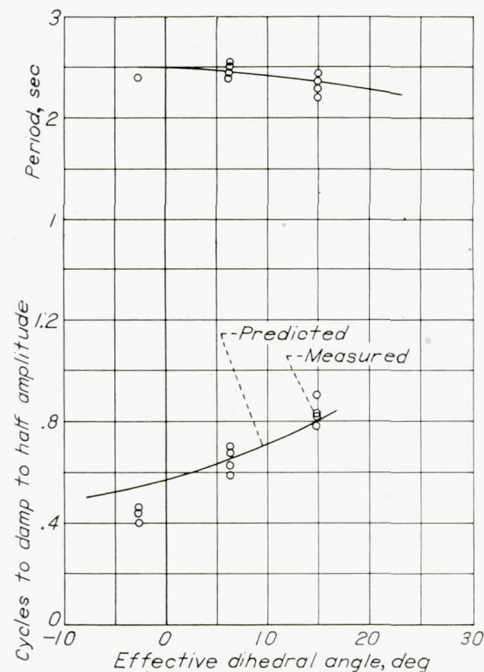


FIGURE 10.—Lateral-oscillation period and damping characteristics.

 $V_1 = 300$  knots.

of  $P$  and  $C_{l\beta}$  predicted by the method of reference 8 are also shown. In general, the best available data on the mass and aerodynamic characteristics were employed in the computations, but minor adjustments were made to give correlation for the normal airplane in order to facilitate comparison of the measured and predicted effects of  $C_{l\beta}$ .

## DISCUSSION

**Characteristics of effective-dihedral control in steady sideslips.**—During steady sideslips, the pilots noted that the apparatus did not cause the airplane to have an artificial feel; that is, it caused no significant difference in the handling characteristics of the airplane from those which would be expected of an airplane with actual dihedral of the magnitudes being simulated by the apparatus. Figure 6 shows desirable smooth and linear variations of pilot-applied aileron deflection and stick force with sideslip angle with the apparatus in operation. The slope of the pilot-applied aileron-deflection curve varies, for the maximum test aileron servo-gearing ratios, from a large stable value to a noticeably unstable value, corresponding to a stick-fixed  $C_{l\beta}$  range from  $-0.0033$  to  $0.0006$  and a  $\Gamma_e$  range from  $14.9^\circ$  to  $-2.7^\circ$ . Since the normal value of  $\Gamma_e$  is  $6.3^\circ$ , the servo action caused about  $\pm 9^\circ$  change. The slope of the stick-force curve varies from a large stable value to approximately zero, indicating large changes in stick-free dihedral effect. However, the force-curve slope is zero when the aileron-deflection-curve slope is unstable; thus, the desired condition that the stick-free  $C_{l\beta}$  and the stick-fixed  $C_{l\beta}$  equal zero at the same gearing ratio was not accomplished for these tests. This condition could be rectified by increasing the tab servo-gearing ratio  $(d\delta_t/d\delta_a)_s$  or the tab effectiveness. The latter solution appeared preferable in the present application because of possible loss in effectiveness of the tab at the large deflections which would result from increases in  $(d\delta_t/d\delta_a)_s$ . The tab chord was increased for the tests reported in part II of this report and the desired results were more closely approximated. The sizable  $\Gamma_e$  range from  $14.9^\circ$  to  $-2.7^\circ$ , which was obtained in these tests, corresponds closely to that originally desired for the investigation of the high-speed dynamic lateral characteristics with the test airplane. However, as more data and experience were gained with the apparatus, the aileron servo-gearing ratio was increased to give about twice the initial  $\Delta\Gamma_e$  of  $\pm 9^\circ$  so that the characteristics of a much wider range of configurations could be studied in part II.

**Characteristics in abrupt rudder kicks.**—The response in roll to a given abrupt rudder deflection is one measure of dihedral effect. The rolling-velocity curves of figure 7 show that, qualitatively, the apparatus successfully simulated large changes in dihedral effect under these severe dynamic conditions; the changes in maximum rolling velocity with servo-gearing ratio (and static  $\Gamma_e$ ) are readily apparent. It is seen that the actual servo-applied aileron deflection is in good agreement with the values computed from the sideslip angle for an ideal servo, except for a time lag of about 0.1 second during the initial portion of the maneuver. The records and computations showed that this time lag did not have a serious effect on the rolling response in simulating positive changes in  $\Gamma_e$  (fig. 7 (b)), but that it caused an undesired initial rolling response when attempting to simulate small negative values of  $\Gamma_e$ . With the apparatus set for  $\Gamma_e = -2.7^\circ$ , the measured response to left rudder deflection showed an initial small left rolling velocity prior to the development of right rolling velocity (fig. 7 (c)). The computed response showed right rolling velocity throughout the maneuver. There was good



agreement, however, between the values of computed and measured maximum rolling velocity and the times at which they occurred. Additional step-by-step response calculations were made, and the results showed that a lag of 0.1 second would account for the undesired initial left roll. Close examination of position-recorder data showed that the lag in servo-applied aileron deflection was due partially to lag in the servo-mechanism response and partially to stretch in the servo-control system between the servo motor and the torque tube. Suitable minor adjustments in the electrical circuit might improve the servo response in future tests. Reduction of the lag due to stretch could be accomplished by a reduction in the flexibility and inertia of the control system, but this would necessitate major changes in the present apparatus.

The effect of this small amount of lag was noticeable to the pilots, but, in their opinion, it did not cause the airplane to have an artificial feel. To the pilots, the small amount of reverse rolling velocity appeared as an effect of yawing velocity, and their opinion was that the apparatus satisfactorily simulated changes in dihedral.

A quantitative measure of the effect of the apparatus in changing the rolling response in abrupt rudder kicks is given by figure 8. The small initial undesired rolling motion at the  $-2.7^\circ$   $\Gamma_e$  setting was ignored in deriving these data. It is seen from figure 8 (a) that the maximum value of the rolling parameter  $pb/2V$  per unit rudder deflection, a measure of dihedral effect, was varied over the wide range from the normal value of 0.005 to 0.011 and  $-0.002$ . Figure 8 (b) shows good agreement between the measured and predicted effects of  $\Gamma_e$  on the rolling response, and thus indicates that the effects of the desired changes in  $\Gamma_e$  are simulated by the apparatus under severe dynamic conditions.

The initial small adverse rolling motion experienced in rudder kicks when the apparatus was used to simulate the  $-2.7^\circ$  value of  $\Gamma_e$  did not prove a serious deficiency in applying the apparatus to the further dynamic-stability studies discussed in part II. This effect was most noticeable when attempting to simulate small negative dihedral effect. As more negative values of  $\Gamma_e$  were obtained by increasing the servo gearing, the initial left rolling velocity following a left rudder kick decreased and the ultimate right rolling velocity increased to the point where the undesired initial motion was not noticeable to the pilot.

**Characteristics in lateral oscillations.**—As was the case for the rudder kicks, the servo-applied aileron deflection lags the sideslip angle a small amount in the lateral-oscillation time histories shown in figures 9 (b) and 9 (c). There are occasional small irregularities in the servo-output motion, but the agreement between actual and ideal aileron deflection is considered good. The time histories show that, qualitatively, the apparatus simulates the effects of changes of  $C_{l\beta}$  on lateral-oscillation characteristics. Compared to the normal characteristics (fig. 9 (a)), the increased excitation of the rolling motion and the decreased damping of the airplane motions caused by an increase in dihedral effect (fig. 9 (b)) are apparent. With a slight negative dihedral effect (fig. 9 (c)), the rolling motion is small, and the airplane motions are rapidly damped.

Fair quantitative agreement between measured and pre-

dicted effects of changes in effective dihedral on oscillation period and damping are shown in figure 10. The discrepancies at the  $-2.7^\circ$  static effective-dihedral-angle setting may be due in part to difficulties in accurately evaluating the oscillation flight data when, as in this case, the damping is high, and due in part to the slight rudder motions which the pilot was unable to eliminate. Both the measured and predicted effects of  $\Gamma_e$  on the period are small. The measured decrease in damping with increasing  $\Gamma_e$  is approximately the same as that given by the predictions, which shows that deviations of the aileron servo characteristics from the ideal did not have a serious effect on the airplane damping.

## II. DETERMINATION OF TOLERABLE RANGE OF EFFECTIVE DIHEDRAL

After the evaluation flights reported in part I the first application of the variable dihedral apparatus was a flight determination of the tolerable range of effective dihedral on the test airplane. As indicated previously, the servo-gearing ratios used for these tests were approximately twice the values used during the tests reported in part I, and the aileron tab was increased in size to give a more favorable relation between stick-fixed and stick-free dihedral effects.

### PROCEDURE

Quantitative data were gathered during steady straight sideslips, rudder-fixed aileron rolls, and lateral oscillations. The lateral oscillations were excited in the same manner as previously discussed in part I.

A survey of pilots' opinions was made among five pilots in a series of flights separate from those during which quantitative measurements were made. Four were NACA test pilots and one was a service pilot; all were highly experienced with fighter-type aircraft. The pilots were requested to report their opinions (in the form of answers to specific questions) with regard to the damping and period of the oscillations, the response to gusts in rough air, their ability to coordinate during turn entries and exits, and the general flying qualities.

The flight conditions chosen for the investigation were as follows:

**Landing-approach condition.**—In this condition the indicated airspeed was 90 knots, the flaps were extended, and the landing gear was retracted. The engine power used was that necessary for level flight. Ninety knots was about the lowest speed at which the servo-applied aileron angle caused by the wings-level sideslip angle was sufficiently small to allow reasonable maneuvers without exceeding the limits of the apparatus. The gear was retracted in order to keep the drag, the propeller loading, and, hence, the wings-level sideslip angle to a minimum.

**Cruising condition.**—The indicated airspeed was 180 knots for this condition; flaps and gear were up. The engine power used was that necessary for level flight. This speed was not so high as to require diving or high engine power for level flight (as was the case at the 300-knot test speed of part I), but it was sufficiently high that further increases in speed would mean only small changes in lift and thrust coefficients.



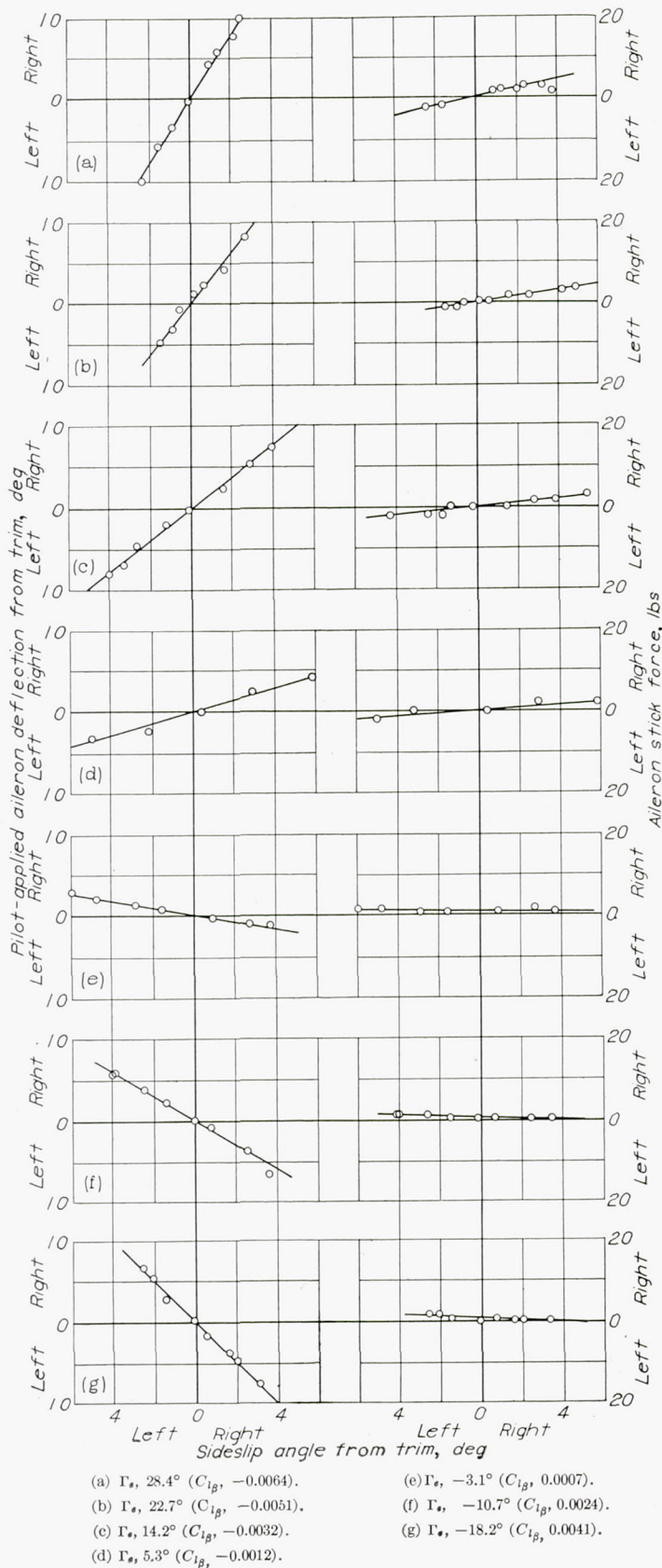


FIGURE 11.—Lateral stability and control characteristics during steady straight sideslips. Landing-approach condition.

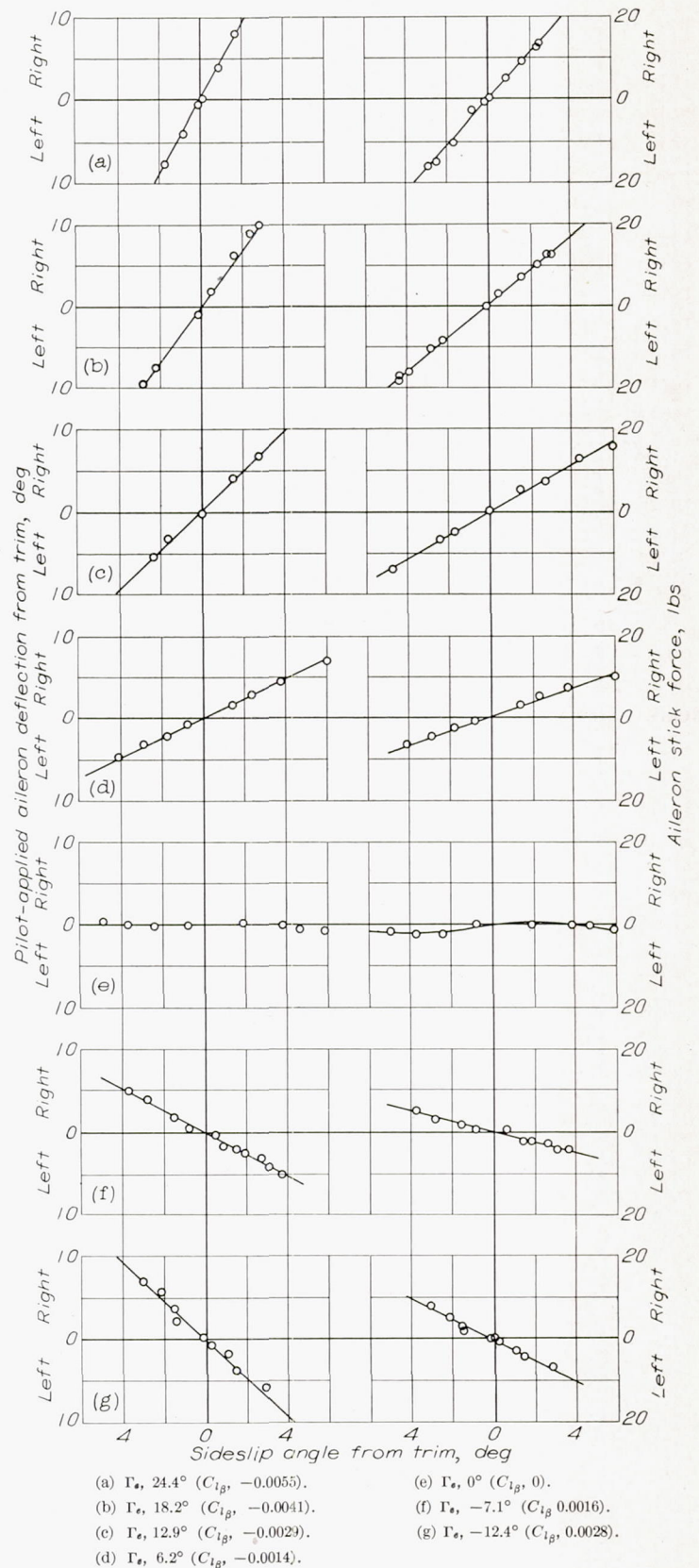


FIGURE 12.—Lateral stability and control characteristics during steady straight sideslips. Cruising condition.



**High-speed condition.**—The indicated airspeed was 250 knots. Flaps and gear were up. It was necessary to fly the airplane in a slight dive at this speed in order to eliminate the necessity of using excessive engine power for long periods. Because of this time-consuming procedure, the testing in this condition was limited to a brief evaluation of the characteristics in steady sideslips and lateral oscillations and of pilots' opinions for three pilots.

All flights were made at a pressure altitude of approximately 7,000 feet. Because of its experimental nature the apparatus was not used in flight close to the ground.

**RESULTS AND DISCUSSION**

**Measurement of the effective dihedral.**—Figures 11 and 12 are presentations of the pertinent data obtained during steady, straight sideslips in the landing-approach and cruising conditions, respectively. Pilot-applied total aileron deflection and aileron stick force are shown as functions of sideslip angle. Since the test speeds during this investigation were lower than those employed in part I, the sideslip angles developed during rudder-fixed aileron rolls (and the associated adverse effect on  $pb/2V$ ) were greater. Hence, the method of evaluating  $C_{l\beta}$  and  $\Gamma_e$  from sideslip data used in part I was not used in evaluating the data of figures 11 and

12. Instead, values of  $C_{l\beta_a}$  for the two test conditions were taken from wind-tunnel tests of a 1/6-scale model of the test airplane, and these values, together with the variations of pilot-applied aileron deflection with sideslip shown in figures 11 and 12, made possible the computation of  $C_{l\beta}$  for each servo setting. The same value of  $C_{l\beta}/\Gamma_e$  of  $-0.000225$  per degree squared used in part I was used to compute the values of  $\Gamma_e$ .

It is seen in figures 11 and 12 that in the landing-approach condition  $\Gamma_e$  was varied from  $-18.2^\circ$  to  $28.4^\circ$ , and in the cruising condition from  $-12.4^\circ$  to  $24.4^\circ$ . The corresponding values of  $C_{l\beta}$  are noted in the figures. The wider range of  $\Gamma_e$  covered in the approach condition as compared with that covered in the cruising condition was caused by higher aileron effectiveness in the approach condition. Sufficient sideslip data (not presented here) were obtained in the high-speed condition to show that  $\Gamma_e$  did not change for a given setting of the apparatus when the airspeed was changed from 180 knots to 250 knots.

**Oscillatory characteristics of the airplane.**—Time histories of typical control-fixed oscillations in the landing-approach condition with the apparatus set for effective dihedrals of  $28.4^\circ$ ,  $5.3^\circ$  (normal airplane, apparatus inoperative), and  $-3.1^\circ$  are shown in figure 13. Figure 14 shows similar time

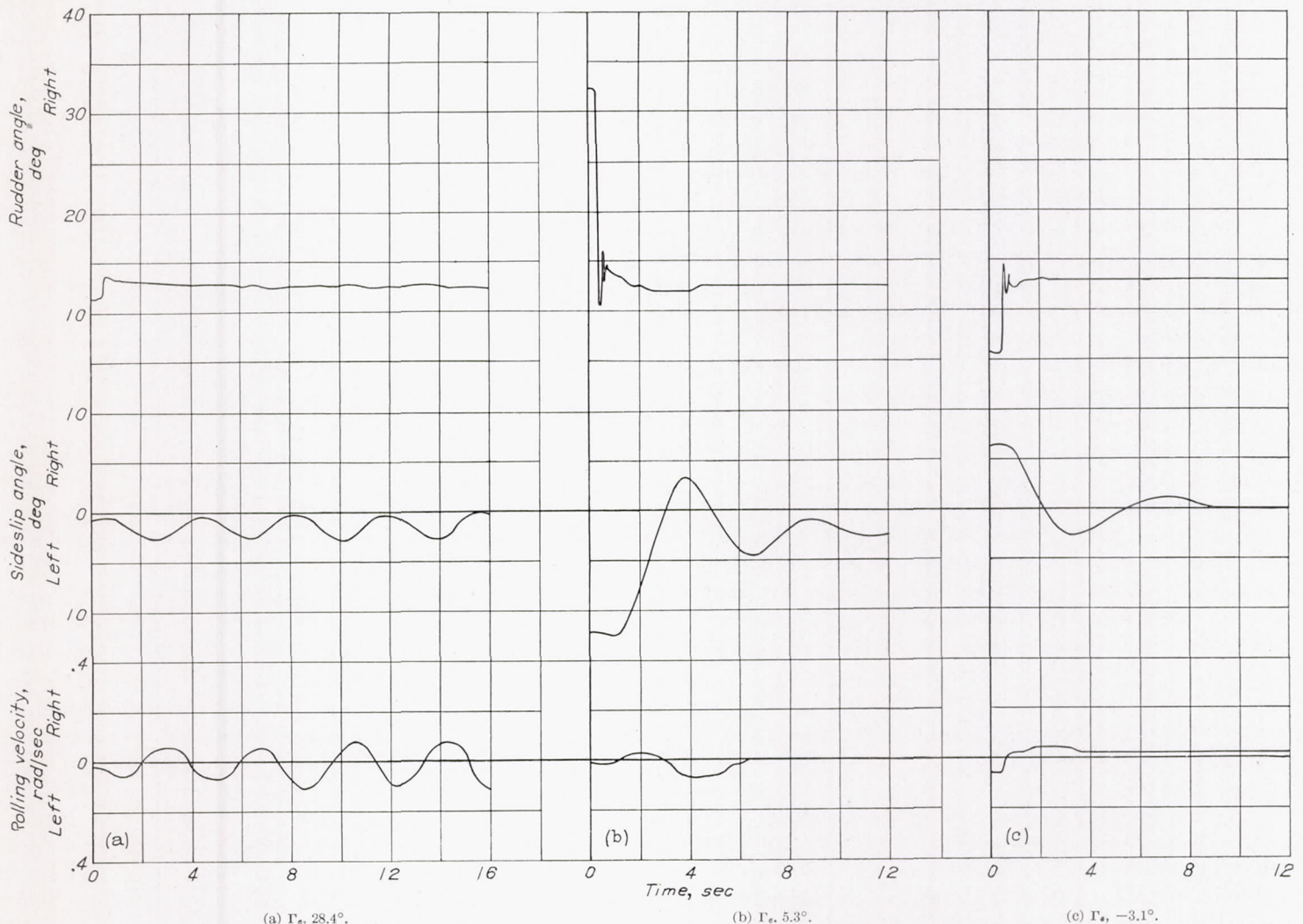


FIGURE 13.—Time histories of typical control-fixed lateral oscillations. Landing-approach condition.



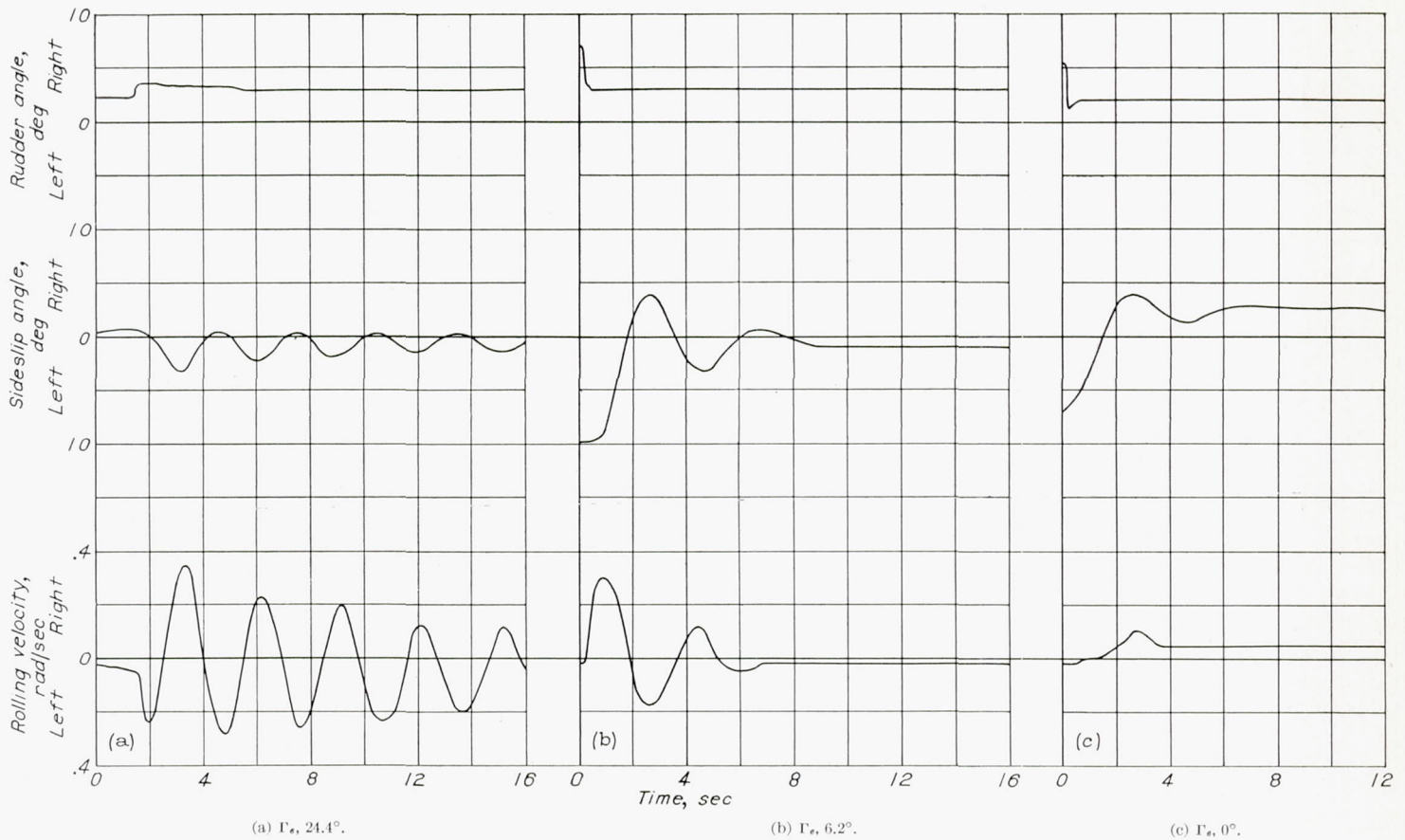


FIGURE 14.—Time histories of typical control-fixed lateral oscillations. Cruising condition.

histories for the cruising condition with effective dihedrals of  $24.4^\circ$ ,  $6.2^\circ$  (normal airplane), and zero. It is seen that, with  $\Gamma_e = 28.4^\circ$  in the approach condition, the airplane exhibited slight oscillatory instability.

The period and damping of oscillations such as those shown in figures 13 and 14 were measured for other dihedral settings and for the high-speed condition. The average values are shown as functions of effective dihedral in figure 15. The time to double amplitude of 38 seconds for the landing-approach condition with  $28.4^\circ$  dihedral is arbitrarily shown in a region of approximately neutral stability. No points are shown for negative  $\Gamma_e$  because, as seen in figure 13, the damping was so high that evaluation of period and damping was virtually impossible.

**Characteristics in rudder-fixed aileron rolls.**—Time histories of typical rudder-fixed aileron rolls for the landing-approach condition with the apparatus set for effective dihedrals of  $28.4^\circ$ ,  $22.7^\circ$ ,  $14.2^\circ$ , and  $5.3^\circ$  (normal airplane with apparatus inoperative) are shown in figure 16. Similar time histories for the cruising condition with effective dihedrals of  $24.4^\circ$ ,  $18.2^\circ$ ,  $12.9^\circ$ , and  $6.2^\circ$  are shown in figure 17. It is seen that rolling-velocity reversals occurred in the landing-approach condition with effective dihedrals greater than that of the normal airplane and in the cruising condition with  $24.4^\circ$  effective dihedral.

Reduction of these data to the conventional plots of the aileron-effectiveness criterion  $pb/2V$  against aileron deflection was not done because the dihedral apparatus is effective over only a limited range of sideslip angle, and the usable aileron deflection during rolls is thereby limited. However,

it was estimated from the available data that the  $pb/2V$  for full aileron deflection would be well below the required value of 0.07 (references 2 and 3) with the high positive dihedrals in the landing-approach condition.

**Pilots' opinions.**—Figure 18 is a graphic summary of the pilots' opinions of the over-all lateral handling characteristics in which pilots' opinions are shown as a function of effective dihedral.

The term "intolerable" as used here means something worse than objectionable, but does not necessarily mean un-flyable. It describes a condition which would be considered dangerous in normal fighter operation.

The term "tolerable" describes a condition which would not be dangerous in normal fighter operation, but which is not necessarily desirable or pleasant.

A "good" condition is not only safe, but is also a desirable or pleasant condition.

The rolling-velocity reversals which occurred in rudder-fixed aileron rolls with high values of effective dihedral (figs. 16 and 17) did not adversely affect the pilots' opinions of the over-all lateral handling characteristics shown in figure 18, although such reversals are unacceptable according to references 2 and 3. One feature of high dihedral which was very desirable to the pilots in the landing-approach condition was the effectiveness of the rudder in producing roll. Thus, for this airplane, the high rate of roll due to the rudder more than offset the low values of rolling velocity, and the reversal in rolling velocity due to aileron deflection. The requirements of references 2 and 3 would, therefore, seem too stringent in this case.



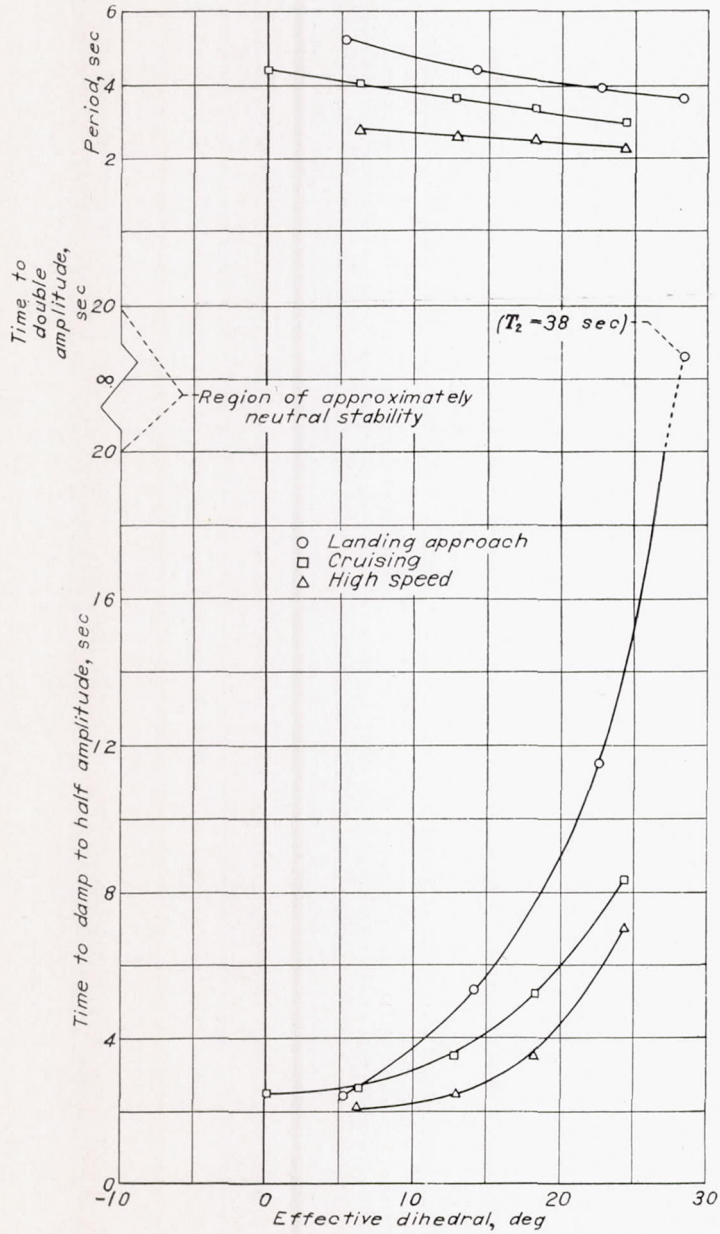
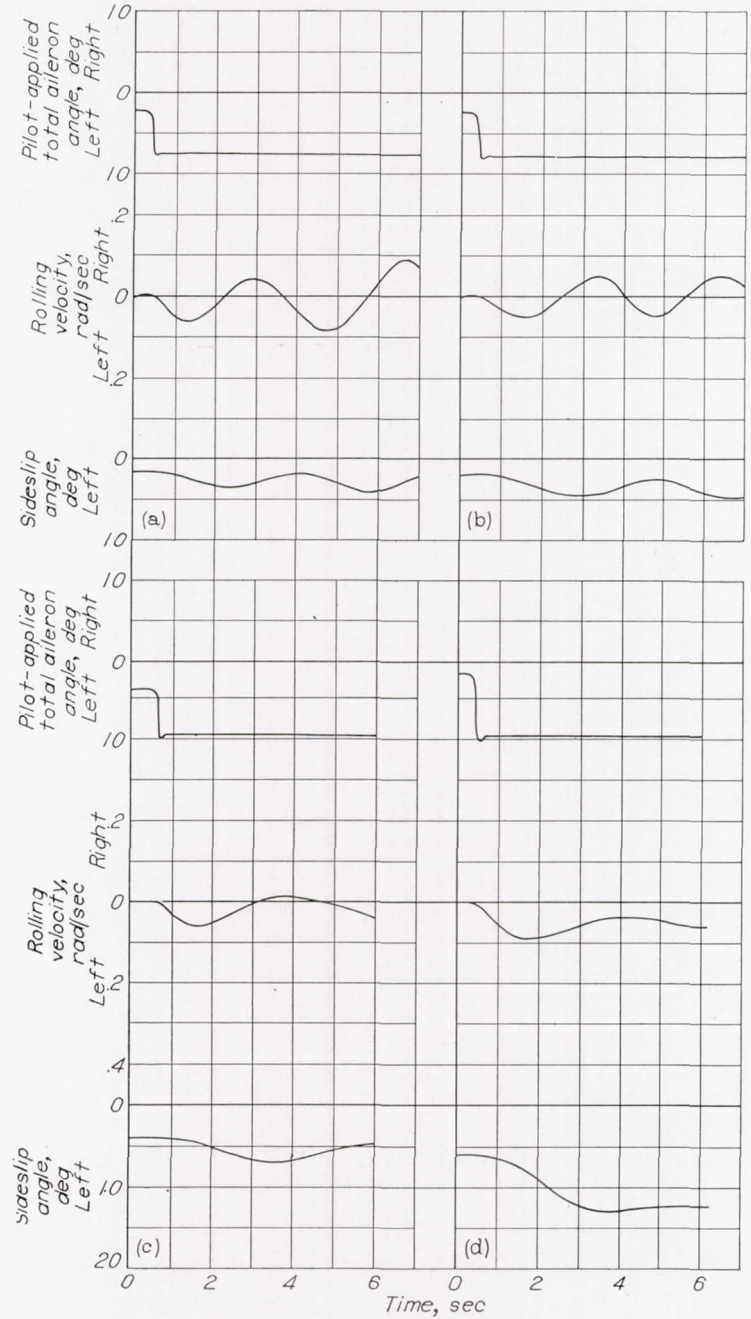


FIGURE 15.—Variation of period and damping of the lateral oscillations with effective dihedral.



(a)  $\Gamma_r, 28.4^\circ$ . (b)  $\Gamma_r, 22.7^\circ$ .  
(c)  $\Gamma_r, 14.2^\circ$ . (d)  $\Gamma_r, 5.3^\circ$  (normal airplane).

FIGURE 16.—Time histories of typical rudder-fixed aileron rolls. Landing-approach condition.



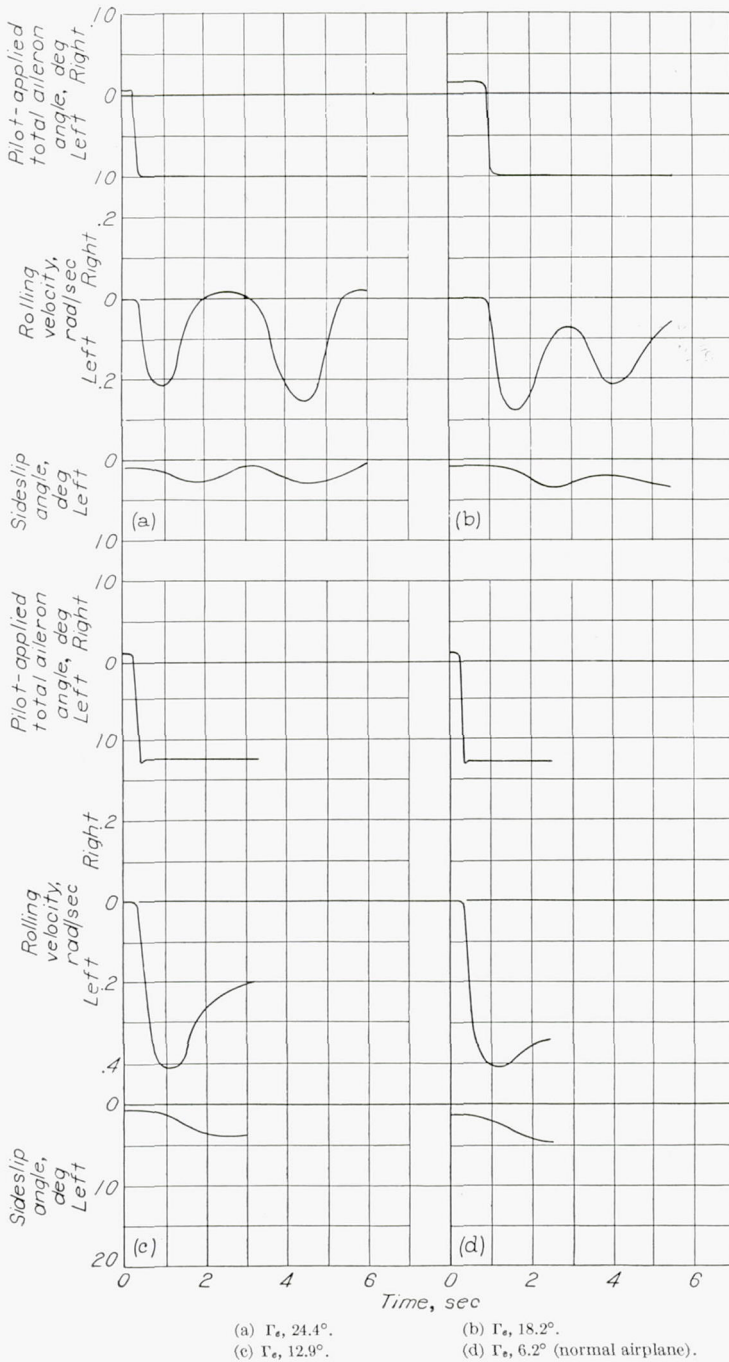


FIGURE 17.—Time histories of typical rudder-fixed aileron rolls. Cruising condition.

Figure 19 shows how the various configurations compare with the period-damping requirements of references 2 and 3. The data of figure 15 were used to plot time to damp to half amplitude against period, and the points were labeled with the opinions shown in figure 18 and the corresponding effective dihedrals.

The maximum tolerable effective dihedral in the landing-approach condition was not reached. Although the highest dihedral used ( $28.4^\circ$ ) produced oscillatory instability in the approach condition, the oscillations were relatively easy to control because, according to the pilots, the period was long and the rolling velocities were not too high. In fact, the pilots considered an effective dihedral of  $22.7^\circ$  to be good in

the approach condition, although the period-damping combination produced by this dihedral (fig. 19) was well within the unsatisfactory area as defined by references 2 and 3. It would appear, then, that the period-damping requirements of references 2 and 3 are too severe in this case.

The maximum tolerable effective dihedral in the cruising and high-speed conditions is seen in figure 18 to be about  $22^\circ$ . Figure 19 shows that, for the cruising condition and the high-speed condition, the good configurations satisfied the requirements of references 2 and 3, but the intolerable configurations did not. With  $24.4^\circ$  effective dihedral in the cruising configuration, the oscillations set up in rough air were difficult to control. Some of the pilots attributed this difficulty to the short period in combination with the low damping. The measurements showed the natural period to be about 3.0 seconds for  $\Gamma_e=24.4^\circ$  in the cruising condition and 3.6 seconds for  $\Gamma_e=28.4^\circ$  in the landing-approach condition. The 3.0-second period in the cruising condition was intolerable, and the 3.6-second period in the approach condition was tolerable—yet the latter was oscillatorily unstable. When presented with the results of the measurements, the pilots agreed that they probably could not detect the difference between a 3.0-second period and a 3.6-second period, at least not definitely enough to enable them to classify one as toler-

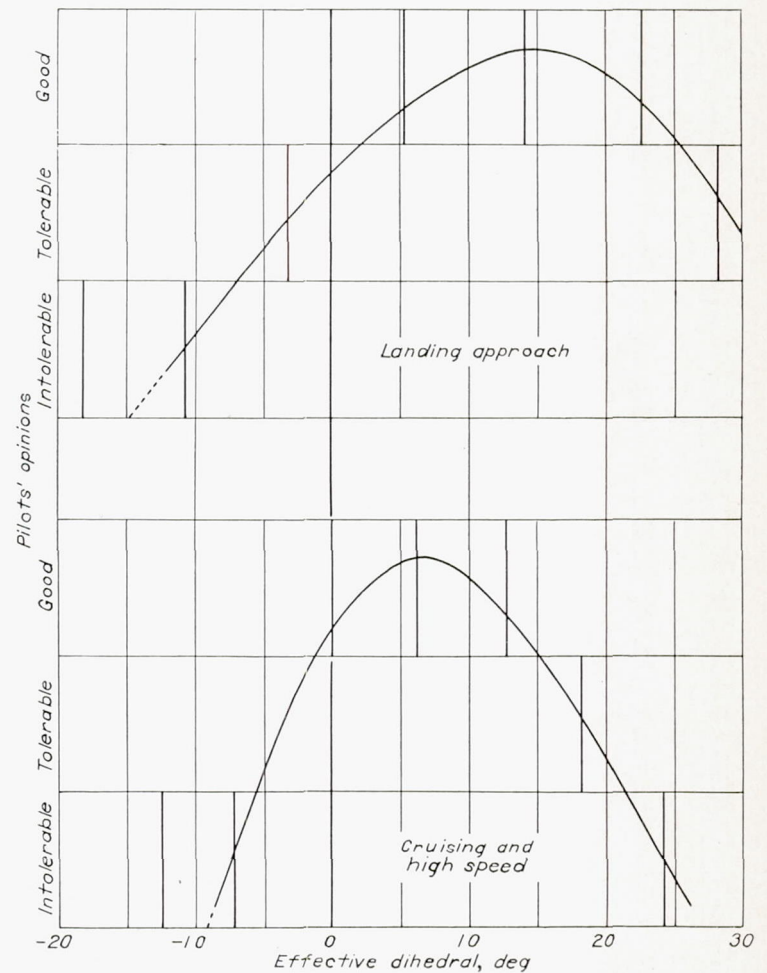


FIGURE 18.—Variation of pilots' opinions of lateral-handling characteristics with effective dihedral.



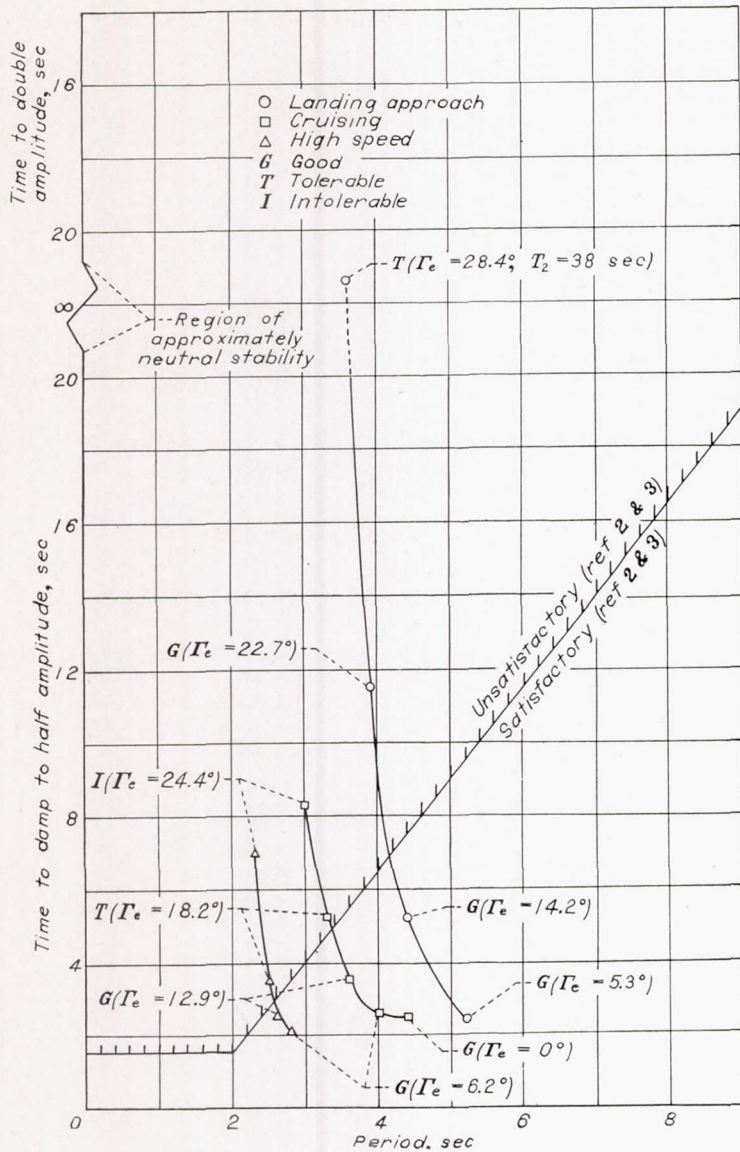


FIGURE 19.—Comparison of pilots' opinions of over-all lateral characteristics with period-damping requirements of references 2 and 3.

able and the other intolerable. The difficulty in controlling the oscillations in the cruising condition was finally attributed by the pilots to the high rolling velocities. These higher rolling velocities are apparent when figure 14 (a) is compared with figure 13 (a). It seems, then, that a period-damping relationship cannot, in itself, define all of a pilot's concepts of the lateral-dynamic-stability characteristics, at least when extreme values of effective dihedral are considered. It would seem that a limitation should be placed on the rolling response to some form of yawing or sideslipping disturbance. The reduction of these concepts to a concrete, numerical criterion is a problem which deserves consideration in future work.

A possible criterion on which a limitation might be placed is the ratio of the amplitude of the rolling velocity to the amplitude of the sideslip angle in the oscillatory mode as measured in lateral oscillations such as were made for this investigation. Another possible criterion worthy of future study is the ratio of the amplitude of angle of bank to that of the angle of sideslip, perhaps as a function of period. For purposes of future reference, the above-mentioned quantities were evaluated from the data gathered during this investiga-

tion and are presented in table I together with the periods, the effective dihedrals, and the pilots' opinions of the over-all lateral handling characteristics.

The minimum tolerable effective dihedral in the landing-approach condition is seen in figure 18 to be about  $-7^\circ$ . With  $\Gamma_e = -10.7^\circ$ , the adverse rolling response to rudder control (left roll with right rudder) was considered by the pilots to be intolerably rapid for a landing approach. It should be noted here, however, that, although all flights were made at altitude, the pilots based their opinions on the consideration of the use of the airplane for field landings. It is believed that, due to lower approach speeds and the necessity for rapid maneuvers during wave-off, the minimum tolerable effective dihedral for carrier landings would be less negative.

The minimum tolerable effective dihedral in the cruising and high-speed conditions is shown in figure 18 to be about  $-5^\circ$ . With  $\Gamma_e = -7.1^\circ$ , the rolling response to gusts and the adverse rolling response to rudder control when corrections were made were so rapid that the pilot had to be constantly on the controls, a situation which, the pilots believed, would be intolerable from the standpoint of fatigue on flights of normal duration.

It was the opinion of the pilots that the optimum values of effective dihedral investigated were  $6.2^\circ$  (normal airplane without apparatus) for the cruising and high-speed conditions and  $14.2^\circ$  for the landing-approach condition. They thought more than normal amounts of dihedral were desirable in the approach condition because of the good response in roll to rudder control. It is noteworthy that this is the direction of the variation of effective dihedral with lift coefficient for swept-back wings; that is, increasing lift coefficient results in increasing effective dihedral.

**Consideration of the results with respect to the flying-qualities specifications.**—Examination of references 2 and 3 indicates that the requirements which probably limit the designer's choice of effective dihedral in most cases are, for the lower limit, the requirement that static effective dihedral be positive and, for the upper limit, the prohibition of rolling-velocity reversal during aileron rolls and the oscillation period-damping requirement (fig. 19). Information gathered during this investigation has indicated that, if these requirements are met with an airplane similar to the test airplane, the resultant lateral-stability characteristics will certainly be satisfactory. The investigation has further indicated, however, that, if necessary, small negative values of effective dihedral can be tolerated and that the upper limit of dihedral is determined by some criterion other than a restriction against rolling-velocity reversal during aileron rolls or a period-damping relationship. The tolerable amount of negative dihedral is apparently related to the growth of rolling motion following a yawing-moment disturbance.

The specific values of the limits of tolerable effective dihedral determined in the present investigation, of course, cannot be applied generally to all airplanes. It is believed that an investigation should be conducted with control over other stability parameters, such as directional stability and directional damping, as well as control over effective dihedral. With such additional control, it would be possible to vary the characteristics of the airplane motion (period, damping,



response, spiral divergence) which seem to be important to the pilots over a much wider range than is possible at present. The formulation of more generally applicable conclusions should thereby be made possible.

### CONCLUSIONS

A flight investigation to evaluate a device for varying effective dihedral and to determine the tolerable (safe for normal fighter operation) limits of effective dihedral at landing-approach, cruising, and high speeds for a conventional fighter airplane resulted in the following conclusions:

1. The device permits large changes in stick-fixed and stick-free dihedral effect to be made readily in flight. The apparatus exhibited a small amount of lag during dynamic maneuvers which, although perceptible to the pilots, was not considered by them to cause any significant change in the feel of the airplane from that of an airplane with similar dihedral.

2. An effective dihedral as high as  $28.4^\circ$  did not cause the airplane to exhibit intolerable stability and control characteristics at landing-approach speed, even though it caused rolling-velocity reversals in rudder-fixed aileron rolls and even though the airplane was oscillatorily unstable. It appears that this was because the period was long, the rolling velocities experienced in rough air were low, and the rudder was very effective in producing roll.

3. The maximum tolerable effective dihedral at cruising and high speeds was indicated to be about  $22^\circ$ . With higher values of dihedral the large and poorly damped rolling motions caused by rough air made the lateral oscillations difficult to control.

4. The minimum tolerable effective dihedral at landing-approach speed was indicated from pilots' opinions formed during flights at altitude to be about  $-7^\circ$  for field landings. With more negative values the adverse rolling response to rudder control (left roll with right rudder) was considered to be dangerously high for an approach.

5. The minimum tolerable effective dihedral at cruising and high speeds was indicated to be about  $-5^\circ$ . With more negative values, the rolling response to gusts and the adverse rolling response to rudder control were so rapid that, in rough air, the pilot had to be constantly on the controls, a situation which was considered dangerous from the standpoint of fatigue for flights of normal duration.

### REFERENCES

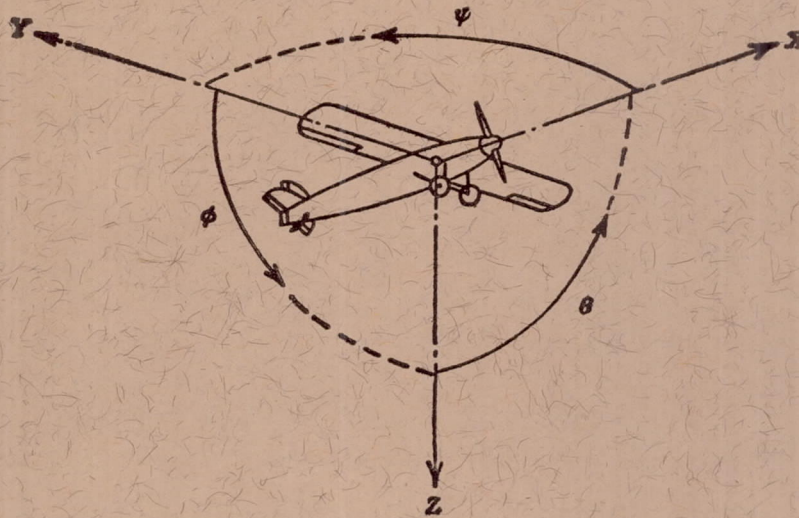
1. Gilruth, R. R.: Requirements for Satisfactory Flying Qualities of Airplanes. NACA Rep. 755, 1943.
2. Anon.: Flying Qualities of Piloted Airplanes. Spec. No. 1815-B, U. S. Air Force, June 1, 1948.
3. Anon.: Specification for Stability and Control Characteristics of Piloted Airplanes. Spec. No. SR-119B, Bur. Aero., Navy Dept., June 1, 1948.
4. Kauffman, William M., Smith, Allan, Liddell, Charles J., Jr., and Cooper, George E.: Flight Tests of an Apparatus for Varying Dihedral Effect in Flight. NACA TN 1788, 1948.
5. Liddell, Charles J., Jr., Van Dyke, Rudolph, D., Jr., and Heinle, Donovan R.: A Flight Determination of the Tolerable Range of Effective Dihedral on a Conventional Fighter Airplane. NACA TN 1936, 1949.
6. Pearson, Henry A., and Jones, Robert T.: Theoretical Stability and Control Characteristics of Wings with Various Amount of Taper and Twist. NACA Rep. 635, 1938.
7. Harper, Charles W., and Jones, Arthur L.: A Comparison of the Lateral Motions Calculated for Tailless and Conventional Airplanes. NACA TN 1154, 1947.
8. Sternfeld, Leonard: Effect of Product of Inertia on Lateral Stability. NACA TN 1193, 1947.

TABLE I.—VALUES OF POSSIBLE CRITERIA FOR LIMITATION OF POSITIVE EFFECTIVE DIHEDRAL AS MEASURED ON THE TEST AIRPLANE

$\Gamma_e$ (deg)	$P$ (sec)	$T_{\frac{1}{2}}$ (sec)	$\left  \frac{p}{\beta} \right $ (per sec)	$\left  \frac{\phi}{\beta} \right $	Pilot opinion
Landing-approach condition					
28.4	3.6	(Unstable, $T_{\frac{1}{2}}=38$ )	3.8	2.3	Tolerable
22.7	3.9	11.5	3.2	2.0	Good
14.2	4.4	5.2	2.1	1.4	Good
5.3	5.2	2.4	0.5	0.4	Good
Cruising condition					
24.4	3.0	8.3	11.2	5.4	Intolerable
18.2	3.3	5.2	9.1	4.7	Tolerable
12.9	3.6	3.5	5.8	3.3	Good
6.2	4.0	2.6	2.3	1.5	Good
High-speed condition					
24.4	2.3	7.0	15.5	5.7	Intolerable
18.2	2.5	3.5	11.5	4.2	Tolerable
12.9	2.6	2.5	7.5	2.7	Good
6.2	2.8	2.1	4.6	1.7	Good

AMES AERONAUTICAL LABORATORY,  
NATIONAL ADVISORY COMMITTEE FOR AERONAUTICS,  
MOFFETT FIELD, CALIF., Aug. 24, 1949.





Positive directions of axes and angles (forces and moments) are shown by arrows

Axis		Force (parallel to axis) symbol	Moment about axis			Angle		Velocities	
Designation	Symbol		Designation	Symbol	Positive direction	Designation	Symbol	Linear (component along axis)	Angular
Longitudinal.....	X	X	Rolling.....	L	Y → Z	Roll.....	φ	u	p
Lateral.....	Y	Y	Pitching.....	M	Z → X	Pitch.....	θ	v	q
Normal.....	Z	Z	Yawing.....	N	X → Y	Yaw.....	ψ	w	r

Absolute coefficients of moment

$$C_l = \frac{L}{qbS}$$

(rolling)

$$C_m = \frac{M}{qcS}$$

(pitching)

$$C_n = \frac{N}{qbS}$$

(yawing)

Angle of set of control surface (relative to neutral position), δ. (Indicate surface by proper subscript.)

#### 4. PROPELLER SYMBOLS

$D$	Diameter
$p$	Geometric pitch
$p/D$	Pitch ratio
$V'$	Inflow velocity
$V_s$	Slipstream velocity
$T$	Thrust, absolute coefficient $C_T = \frac{T}{\rho n^2 D^4}$
$Q$	Torque, absolute coefficient $C_Q = \frac{Q}{\rho n^2 D^5}$

$P$	Power, absolute coefficient $C_P = \frac{P}{\rho n^3 D^5}$
$C_s$	Speed-power coefficient $= \sqrt[5]{\frac{\rho V^5}{P n^2}}$
$\eta$	Efficiency
$n$	Revolutions per second, rps
$\Phi$	Effective helix angle $= \tan^{-1} \left( \frac{V}{2\pi r n} \right)$

#### 5. NUMERICAL RELATIONS

1 hp = 76.04 kg-m/s = 550 ft-lb/sec  
 1 metric horsepower = 0.9863 hp  
 1 mph = 0.4470 mps  
 1 mps = 2.2369 mph

1 lb = 0.4536 kg  
 1 kg = 2.2046 lb  
 1 mi = 1,609.35 m = 5,280 ft  
 1 m = 3.2808 ft